

THIRD PARTY RESEARCH. PENDING FAA REVIEW.



**Small UAS Detect and Avoid Requirements Necessary for
Limited Beyond Visual Line of Sight (BVLOS) Operations:
Task 6 UND September 2020 Flight Test Report**

February 7, 2022

NOTICE

This document is disseminated under the sponsorship of the U.S. Department of Transportation in the interest of information exchange. The U.S. Government assumes no liability for the contents or use thereof. The U.S. Government does not endorse products or manufacturers. Trade or manufacturers' names appear herein solely because they are considered essential to the objective of this report. The findings and conclusions in this report are those of the author(s) and do not necessarily represent the views of the funding agency. This document does not constitute FAA policy. Consult the FAA sponsoring organization listed on the Technical Documentation page as to its use.

LEGAL DISCLAIMER

The information provided herein may include content supplied by third parties. Although the data and information contained herein has been produced or processed from sources believed to be reliable, the Federal Aviation Administration makes no warranty, expressed or implied, regarding the accuracy, adequacy, completeness, legality, reliability or usefulness of any information, conclusions or recommendations provided herein. Distribution of the information contained herein does not constitute an endorsement or warranty of the data or information provided herein by the Federal Aviation Administration or the U.S. Department of Transportation. Neither the Federal Aviation Administration nor the U.S. Department of Transportation shall be held liable for any improper or incorrect use of the information contained herein and assumes no responsibility for anyone's use of the information. The Federal Aviation Administration and U.S. Department of Transportation shall not be liable for any claim for any loss, harm, or other damages arising from access to or use of data or information, including without limitation any direct, indirect, incidental, exemplary, special or consequential damages, even if advised of the possibility of such damages. The Federal Aviation Administration shall not be liable to anyone for any decision made or action taken, or not taken, in reliance on the information contained herein.

Technical Report Documentation Page

1. Report No. DOT/FAA/AR-xx/xx		2. Government Accession No.		3. Recipient's Catalog No.	
4. Title and Subtitle TITLE OF REPORT Small UAS Detect and Avoid Requirements Necessary for Limited Beyond Visual Line of Sight (BVLOS) Operations: Task 6 UND September 2020 Flight Test Report				5. Report Date February 7, 2022	
				6. Performing Organization Code ASSURE: University of North Dakota	
7. Author(s) Mark Askelson				8. Performing Organization Report No.	
9. Performing Organization Name and Address University of North Dakota Tech Accelerator Room 2050 4201 James Ray Dr Stop 8367 Grand Forks, ND 58202-8367				10. Work Unit No. (TRAIS)	
				11. Contract or Grant No. 15-C-UAS	
12. Sponsoring Agency Name and Address U.S. Department of Transportation Federal Aviation Administration Washington, DC 20591				13. Type of Report and Period Covered Interim Report	
				14. Sponsoring Agency Code	
15. Supplementary Notes					
16. Abstract <p>The demand for Beyond Visual Line Of Sight (BVLOS) operations using small Unmanned Aircraft Systems (sUASs) is high. A major impediment to realization of these operations is the Detect And Avoid (DAA) function. Two critical DAA challenges are definition of sUAS DAA system performance requirements and development of test methods for those performance requirements. The ASTM (American Society for Testing and Materials) WK62668 Detect and Avoid Performance Requirements Task Group has developed proposed performance requirements for sUAS DAA. The ASTM WK62669 DAA Test Methods Task Group is currently developing test methods for evaluating compliance of sUAS DAA systems with performance requirements. This effort is informing the ASTM WK62669 DAA Test Methods Task Group.</p> <p>A flight test method that is part of a broader testing approach that also involves simulation, lab testing, etc., is described herein. This test method leverages a geometric approach to gathering data, in which potential encounter geometries are varied. Justification for the subset chosen herein, including how it relates to the broader set of encounters, is provided.</p> <p>Numerous metrics are developed and evaluated. These include sample risk ratio (from the DAA performance standard) and sample risk ratio uncertainty, which provides insight into whether the proposed approach (number of encounters) provides a viable basis for evaluation of risk ratio. In addition, encounter events (well clear/horizontal well clear/vertical well clear violations) are presented, overall encounter metrics such as Closest Point of Approach (CPA) are evaluated, and metrics for the major stages of DAA are proposed and presented. Maintenance of well clear status during testing, which is a goal during testing, is also evaluated.</p> <p>For the encounter set that was evaluated, the sample risk ratio uncertainty, which was evaluated using three different methods, indicates that the set is viable for providing guidance regarding conformance with the performance standard. This performance must be placed in context with the broader set of encounters, the breadth of which can be evaluated through simulation. Moreover, the metrics that are developed herein for the major stages of DAA, which were developed through the need for information regarding how the system is performing and qualified by pragmatic considerations (e.g., timing challenges associated with data collection), provide useful information regarding these major stages (and are being considered by the ASTM WK62669 DAA Test Methods Task Group). Finally, methods developed for analyzing encounters, which include visualization techniques and summary metrics, enable understanding of encounter characteristics.</p>					
17. Key Words Test Plan Detect and Avoid Standards			18. Distribution Statement This document is available to the U.S. public through the National Technical Information Service (NTIS), Springfield, Virginia 22161. This document is also available from the Federal Aviation Administration William J. Hughes Technical Center at actlibrary.tc.faa.gov .		
19. Security Classif. (of this report) Unclassified		20. Security Classif. (of this page) Unclassified		21. No. of Pages 84	22. Price

TABLE OF CONTENTS

TECHNICAL REPORT DOCUMENTATION PAGE	IV
TABLE OF CONTENTS	V
TABLE OF FIGURES	VII
TABLE OF TABLES	VIII
TABLE OF ACRONYMS	IX
EXECUTIVE SUMMARY	X
1 INTRODUCTION	1
2 TEST PLAN	1
2.1 BACKGROUND.....	1
2.1.1 Standards Efforts.....	1
2.1.2 Encounter Characteristics.....	2
2.1.2.1 Geometries	5
2.1.2.2 Speed Variations	5
2.1.2.3 Considerations for LR	6
2.2 TEST OBJECTIVES.....	8
2.3 TEST PERSONNEL.....	8
2.3.1 NPUASTS.....	8
2.3.2 UND.....	8
2.3.3 SkySkopes (UAS Operator).....	9
2.3.4 L3 Harris Technologies.....	9
2.3.5 Distribution and Roles.....	9
2.4 DAA SYSTEM.....	12
2.5 TEST AIRCRAFT.....	15
2.6 TEST LOCATIONS.....	15
2.6.1 Locations of Test Elements.....	15
2.6.2 Georeferenced Encounter Geometry Generation.....	19
2.7 TEST DATES AND SCHEDULE.....	21
2.8 TEST CONDITIONS.....	22
2.9 TEST CARDS.....	22
2.10 DATA COLLECTION AND MANAGEMENT.....	23
2.10.1 Metadata.....	23
2.10.2 DCAPS.....	24
2.10.3 Aircraft Position Truth Data.....	27
2.10.4 Additional Data Sets.....	28

3	DATA ANALYSIS	28
3.1	METRICS	28
3.1.1	<i>Individual Encounter Metrics</i>	28
3.1.1.1	Encounter Events	28
3.1.1.2	Encounter Descriptors	29
3.1.1.3	Distance Metrics	30
3.1.1.4	Summary and DAA Steps	31
3.1.1.5	Separation Timeline	39
3.1.1.5.1	2D (Horizontal) Unmitigated CPA (CPA _h) Derivation	39
3.1.1.5.2	3D Unmitigated CPA Derivation	40
3.1.1.5.3	Evaluation of Unmitigated CPA _h Accuracy	41
3.1.2	<i>Campaign Metrics</i>	42
3.1.2.1	(Sample) Risk Ratio	42
3.1.2.2	Sample Risk Ratio Uncertainty	43
3.1.2.2.1	Non-Homogeneous	43
3.1.2.2.2	Homogeneous	46
3.2	SOFTWARE	47
3.2.1	<i>Language</i>	47
3.2.2	<i>Organization</i>	47
3.2.2.1	ByDay Software	47
3.2.2.2	Campaign Software	48
4	TEST RESULTS	49
4.1	FLIGHT SUMMARY	49
4.2	ENCOUNTER EVENTS.....	49
4.3	VERTICAL SEPARATION INTEGRITY	52
4.4	EXAMPLE ENCOUNTERS	54
4.5	SAMPLE RISK RATIO AND SAMPLE RISK RATIO UNCERTAINTY	59
5	CONCLUSIONS	63
5.1	LESSONS LEARNED	63
5.2	UTILIZATION IN ASTM WK62669 DAA TEST METHODS TASK GROUP	64
5.3	FUTURE WORK.....	64
5.4	SUMMARY.....	64
	BIBLIOGRAPHY	67
	APPENDIX A: HIGH-LEVEL OVERVIEW OF TEST PROCESS	70
	APPENDIX B: TEST CARDS/SCRIPTS FOR UND/NPUASTS 21-25 SEPTEMBER 2020 TESTS	74

TABLE OF FIGURES

Figure 1. Illustration of encounter geometry angles.	6
Figure 2. Personnel distribution, systems, and data sources for core September 2020 flight test capabilities.	10
Figure 3. The C Speed Lightwave Radar utilized during the September 2020 flight tests.	14
Figure 4. Locations of testing elements during the September 2020 flight tests.	17
Figure 5. Sectional centered on the September 2020 flight test area.	18
Figure 6. Images from the Lovas farm.	19
Figure 7. Illustration of encounters associated with the MA flying northwest to southeast.	20
Figure 8. As in Figure 7 but for the MA flying southeast to northwest.	21
Figure 9. Schedule for a nominal test day.	22
Figure 10. Spreadsheet utilized to capture test metadata.	24
Figure 11. GCS DCAPS interface.	25
Figure 12. EO DCAPS interface.	26
Figure 13. FTD DCAPS interface.	27
Figure 14. Illustration of the difference between a Normal and Truncated Normal distribution.	45
Figure 15. Illustration of best-case and worst-case Truncated Normal distributions.	46
Figure 16. Encounter events for the September 2020 flight test encounters.	52
Figure 17. Box-and-whisker plots of aircraft AGL altitudes and aircraft altitude differences for 22 September 2020.	54
Figure 18. Box-and-whisker plots of aircraft AGL altitudes and aircraft altitude differences for 25 September 2020.	54
Figure 19. Illustration of the 154437-154653 UTC 23 September 2020 encounter.	57
Figure 20. Illustration of the 155014-155210 UTC 23 September 2020 encounter.	58
Figure 21. Illustration of the 155857-160034 UTC 23 September 2020 encounter.	59
Figure 22. Box and whisker plots of CPA_h for the encounter geometries for each intruder speed.	61
Figure 23. Cumulative Density Functions (CDFs) of CPA_h for the encounter geometries for each intruder speed.	62
Figure A1. Illustration for an HE_0 scenario.	73

TABLE OF TABLES

Table 1. DAA performance guidance from ASTM (2020).	2
Table 2. Summary of very low level manned aircraft operations from Weinert and Barrera (2020).	4
Table 3. UND-NPUASTS September 2020 test partners.	8
Table 4. Information regarding the L3Harris™ DAA system.	13
Table 5. Information regarding the UA used during the September 2020 flight tests.	15
Table 6. Information regarding the intruder aircraft used during the September 2020 flight tests.	15
Table 7. Origination points for the UA and MA used during the September 2020 flight tests.	23
Table 8. GPS errors.	27
Table 9. Summary data for 23 September 2020 encounters.	33
Table 10. OEP Summary data for 23 September 2020 encounters.	34
Table 11. Detect (D) step data for 23 September 2020 encounters.	35
Table 12. Track (T) step data for 23 September 2020 encounters.	36
Table 13. Evaluate (E) step data for 23 September 2020 encounters.	37
Table 14. Maneuver (M) step data for 23 September 2020 encounters.	38
Table 15. Examples of CPA _{<i>h</i>} errors from the September 2020 flight tests.	42
Table 16. Summary of September 2020 flight test encounters.	49
Table 17. Summary data for 22 September 2020 encounters.	51
Table 18. Comparison of LR_{ch} values and uncertainty windows.	63

TABLE OF ACRONYMS

Acronym	Meaning
2D	Two-Dimensional
A&G	Alerting and Guidance
A1F	Alert Function
A2F	Avoid Function
ADS-B	Automatic Dependent Surveillance-Broadcast
AGL	Above Ground Level
ASTM	American Society for Testing and Materials
BVLOS	Beyond Visual Line Of Sight
CDF	Cumulative Density Function
CFR	Code of Federal Regulations
CPA	Closest Point of Approach
DAA	Detect And Avoid
DCAPS	Data Collection and Processing System
DF	Detect Function
DTEM	Detect, Track, Evaluate, and Maneuver
DVR	Digital Video Recorder
FAA	Federal Aviation Administration
FoV	Field of View
FTD	Flight Test Director
FTR	False Target Rating
GBDAA	Ground Based Detect And Avoid
GCS	Ground Control System
GPS	Global Positioning System
HEFP	Horizontal Encounter Focal Point
HITL	Human In The Loop
LRE	Launch and Recovery Element
LTE	Long-Term Evolution
MA	Manned Aircraft
MC	Mission Commander
MSU	Mississippi State University
NMAC	Near Mid-Air Collison
NPUASTS	Northern Plains UAS Test Site
OEP	Objective Encounter Period
PDF	Probability Density Function
PI	Principal Investigator
PIC	Pilot in Command
SBS	Surveillance and Broadcast Services
SBSS	Surveillance and Broadcast Services Subsystem
SPS	Standard Positioning Service
sUAS	Small Unmanned Aircraft System
SWaP	Size, Weight, and Power
UA	Unmanned Aircraft
UAS	Unmanned Aircraft System
UND	University of North Dakota
UPS	Uninterruptable Power Supply
UTC	Universal Time Coordinated
VAS	Value Added Service
VHF	Very High Frequency
WAAS	Wide Area Augmentation System
WCV	Well Clear Violation

EXECUTIVE SUMMARY

The demand for Beyond Visual Line Of Sight (BVLOS) operations using small Unmanned Aircraft Systems (sUASs) is high. A major impediment to realization of these operations is the Detect And Avoid (DAA) function. Several challenges exist for sUAS DAA. Of these, two critical challenges are definition of sUAS DAA system performance requirements and development of test methods for those performance requirements. The ASTM (American Society for Testing and Materials) WK62668 DAA Performance Requirements Task Group has developed proposed performance requirements for sUAS DAA. The ASTM WK62669 DAA Test Methods Task Group is currently developing test methods for evaluating compliance of sUAS DAA systems with performance requirements. This effort is informing the ASTM WK62669 DAA Test Methods Task Group. In addition, as part of the project “A18_ A11L.UAS.22 – Small UAS Detect and Avoid Requirements Necessary for Limited Beyond Visual Line of Sight (BVLOS) Operations: Separation Requirements and Testing” (A18), this report also describes development of a test plan for sUAS DAA systems and evaluation of that test plan. The fundamental questions are:

- How can flight tests be designed to provide the needed information for evaluation of compliance with DAA performance requirements? How much testing (how many encounters) is (are) needed?
- How can flight tests be designed to ensure safety during the testing process?
- What data elements are needed for evaluation of compliance with performance requirements?

This report describes a flight test method that is part of a broader testing approach that also involves simulation, lab testing, etc. This test method leverages a geometric approach to gathering data, in which potential encounter geometries are varied.¹ At present, the team has evaluated horizontal encounters, as they continue to develop a safe means for testing descend- and climb-into encounters. Pragmatic drivers, including time and cost, result in a subset of the total number of possible encounters being evaluated. The report explains the justification for the subset chosen, including how it relates to the broader set of encounters. Based upon this work, the team has proposed a method for relating the results derived from this subset to simulation-based results as part of an overall test method approach to the ASTM WK62669 DAA Test Methods Task Group. Currently, this is a major challenge faced by this group—how to validate simulations using flight tests data.

The team developed and evaluated numerous metrics. These include sample risk ratio (from the DAA performance standard) and sample risk ratio uncertainty, which provides insight into whether the proposed approach (number of encounters) provides a viable basis for evaluation of risk ratio. In addition, the team presented encounter events (well clear/horizontal well clear/vertical well clear violations), evaluated overall encounter metrics such as Closest Point of Approach (CPA), and proposed and presented metrics for the major stages of DAA. The team also evaluated maintenance of well clear status during testing, which is a goal during testing.

¹ Limited evaluation of speed variations is also performed.

For test methodology, the team initially used a vertical aircraft altitude safety offset of 350 ft during these tests which generally ensured maintenance of well clear status during the tests. Three minor well clear violations occurred, however. Based upon this, the researchers recommend a 400 ft vertical aircraft altitude safety offset for horizontal encounters. Moreover, the team recommends closer monitoring of intruder altitudes during testing to ensure that the intruder is operating at the desired altitude.

For the encounter set that was evaluated, the sample risk ratio uncertainty, evaluated using three different methods, indicates that the set provides viable guidance regarding conformance with the performance standard. An evaluator must place this performance in context with the broader set of encounters, the breadth of which can be evaluated through simulation. Moreover, the metrics that are developed herein for the major stages of DAA, which were developed through the need for information regarding how the system is performing and qualified by pragmatic considerations (e.g., timing challenges associated with data collection), provide useful information regarding these major stages (and are being considered by the ASTM WK62669 DAA Test Methods Task Group). Finally, methods developed for analyzing encounters, including visualization techniques and summary metrics, enable understanding of encounter characteristics. This includes the situation wherein aircraft closure rates increase for a period of time after maneuver initiation.

This report provides identifies topics deserving of further evaluation. These include addition of other variations in flight tests (curved trajectories, climb/descend-into encounters, etc.) and impacts of expanding the number of encounters upon uncertainties. Some future research directions will likely arise as the ASTM WK62669 DAA Test Methods Task Group continues to integrate these findings into its standard.

1 INTRODUCTION

One of the fundamental tasks in this project, “A18_ A11L.UAS.22 – Small UAS Detect and Avoid Requirements Necessary for Limited Beyond Visual Line of Sight (BVLOS) Operations: Separation Requirements and Testing” (A18), is development of a test plan for sUAS (small Unmanned Aircraft System) Detect And Avoid (DAA) systems and evaluation of that test plan. This report describes the tests conducted at the University of North Dakota (UND) by the UND and Northern Plains UAS Test Site (NPUASTS) during the week of 20-26 September 2020. This includes the test plan, test results, and lessons learned.

2 TEST PLAN

Below, UND provides an overview of the test plan. The reader is referred to the overarching A18 test plan “Small UAS Detect and Avoid Requirements Necessary for Limited Beyond Visual Line of Sight (BVLOS) Operations: Separation Requirements and Testing: (Overarching) Test Plan” and the specific test plan for this event “ASSURE A18 NPUASTS Test Plan Revision 3” for more details.

2.1 Background

2.1.1 Standards Efforts

Two ASTM (American Society for Testing and Materials) groups, the ASTM WK62668 Detect and Avoid Performance Requirements Task Group and the ASTM WK62669 DAA Test Methods Task Group, are actively developing standards for sUAS DAA. The ASTM WK62668 DAA Performance Requirements Task Group has published a performance requirements standard (ASTM 2020). These performance requirements apply to Low Air Risk and Medium Air Risk operational volumes, which are operational volumes that are defined according to air collision risk. The defined categories are:

- High Air Risk: This is airspace where manned aircraft predominately fly and/or the manned aircraft encounter rate is frequent. The competent authority is expected to require the operator to comply with recognized DAA system standards as available and appropriate to the application.
- Medium Air Risk: This is airspace where manned aircraft predominately do not fly (excluding helicopters and crop dusters) and/or the Manned Aircraft (MA) encounter rate is occasional. This is generally uncontrolled airspace and/or airspace that extends from the ground to between 300 ft to 1,200 ft AGL (with 500 ft AGL used as a common default) above which most MA operations are conducted. This includes airspace away from Class B, C, D aerodromes, or near Class B, C, D aerodromes with additional strategic mitigations.
- Low Air Risk: This is airspace where manned aircraft predominately do not fly (excluding helicopters and crop dusters) and/or the MA encounter rate is remote or improbable in accordance with guidelines from the competent authority. This is generally uncontrolled airspace and/or airspace that extends from the ground to between 300 ft to 1,200 ft AGL (with 500 ft AGL used as a common default) above which most manned aircraft operations are conducted, and away from urban populations centers, towns, outer suburban, suburban, residential areas, metro, or cities, and outside all aerodromes.

- **Extremely Low Air Risk:** This is airspace where MA predominately do not fly and/or the MA encounter rate is extremely improbable. It is generally defined as airspace where the risk of collision between a UAS and MA is acceptable without the addition of any tactical mitigation (e.g., a DAA system). An example of this may be UAS flight operations in some parts of Alaska or northern Sweden where the MA density is so low that the airspace safety threshold could be met without any mitigation.

ASTM (2020) defined (logic) risk ratio performance requirements for Low Air Risk and Medium Air Risk operational volumes.² These are provided in Table 1.

Table 1. DAA performance guidance from ASTM (2020).

Intruder Equipage	NMAC (Near Mid-Air Collision) Risk Ratio (RR)	Well Clear Risk Ratio (LR)
Transponder or ADS-B Out	≤ 0.18	≤ 0.40
Non-Cooperative	≤ 0.30	≤ 0.50

2.1.2 *Encounter Characteristics*

From an encounter/trajectory standpoint, intruder aircraft can exhibit variations in the following (hereinafter four dimensions of variability):

- Horizontal direction
- Vertical direction (e.g., climb/descend)
- Horizontal speed
- Vertical speed/rate

These are generally considered to be ground-relative (e.g., ground-relative speed) and, of course, are components of the (ground-relative) aircraft velocity. By varying these, all types of encounter trajectories can be generated (straight, curved, curved with changes in horizontal speed, ascending, descending, curved with descent, etc.).

Traditionally, data regarding MA behavior has been characterized using encounter models (e.g., (Edwards et al. 2009; Griffith et al. 2013; Weinert et al. 2013; Underhill et al. 2018; Weinert et al. 2018). Such models have evolved such that aircraft characteristics are updated each second (Weinert et al. 2013). Given such models, typical flight patterns could be extracted, with any erratic (if present) and presumably less likely patterns not being used unless they represent a significant challenge for DAA systems. However, given the lack of MA data for very low-level flights (Weinert et al. 2019), such an encounter model does not exist. Weinert et al. (2019) is

² Risk ratio is, generally, the likelihood of an event. In this context, the loss of well clear risk ratio, for example, is the ratio of the likelihood of the loss of well clear with use of a DAA system given an encounter set and the likelihood of loss of well clear without the use of a DAA system for that encounter set. See ASTM (2020).

working to develop a model using ADS-B (Automatic Dependent Surveillance-Broadcast) data from the OpenSky network (Schäfer et al. 2014).

Given that a statistical encounter model for manned flight at very low levels is not available, a heuristic model based upon intruders that commonly operate at very low levels is used instead. Weinert and Barrera (2020) provide an extensive review of very low-level manned operations. As indicated by Weinert and Barrera (2020), numerous manned operations occur at very low levels (Table 2). Away from offshore areas, flight schools, specific tourist attractions, and urban areas (helicopter news and public safety), the most common operation is expected to be spraying and dusting.

Spraying and dusting operations consist of five types of flight “legs”:

- Takeoff and landing
- Transition to and from the field being sprayed
- Application leg
- Ascent at the end of an application leg
- Descent into an application leg.

During the transition and application legs, the MA is generally in straight, level flight. During takeoff and landing, ascent at the end of an application leg, and descent into an application leg, the MA is ascending and descending and, during the last two legs, turning. Because a sUAS could encounter such an aircraft during any of these flight legs, testing of sUAS DAA systems should include both horizontal encounters and encounters where the intruder is approaching from above and below.

Table 2. Summary of very low-level manned aircraft operations from Weinert and Barrera (2020).

Operation	Flight Altitudes (ft AGL)	Speeds (kts)	Comments
Spraying and Dusting	2-20	50-120	
Insect Release	300-2500	78-88*	
Fish Release	150-300	70	
Helicopter Air Ambulance	0 and up	Not Provided	
Helicopter Air Tours	400-3300	Not Provided	Aircraft models can be used to obtain airspeeds.
Helicopter Offshore Operations	500 and up	Not Provided	Aircraft models can be used to obtain airspeeds.
Training	500 and up**	Not Provided	Aircraft models can be used to obtain airspeeds.
Animal Sciences	30-4590***	19-175****	
Earth Sciences	100-2130	27-120	
Plant Sciences	<500-32,000	11-200	
Helicopter News and Public Safety	500-3280	0-140	

*Average speeds based on operational guidance.

**Based on regulations.

***Many operations are reported to occur below 500 ft AGL.

****175 kt flights at altitudes 1200-2000 ft AGL. Highest speed for altitudes < 700 ft AGL is 108 kts.

Away from offshore areas, flight schools, specific tourist attractions, and urban areas, helicopter air ambulance operations are arguably the second most common very low-level MA operation. While the exact altitudes at which such aircraft are flown when transiting to and from an accident site are not known, it is expected that such legs could be conducted at altitudes below 500 ft AGL and, by regulation (§135.203 of the Code of Federal Regulations), 300 ft above the surface (e-CFR 2021a). In addition, such flights include ascent and descent in locations where encounters with sUAS may occur. Thus, both horizontal encounters and encounters where this type of intruder approaches from above and below are needed when testing sUAS DAA systems.

For the rest of the operations in Table 2, horizontal encounters with sUAS are expected to dominate the encounter set. It is noted that because helicopter air tours and helicopter news and safety flights

can involve the MA hovering, such encounters include closure rates that are purely driven by sUAS flight speeds.

2.1.2.1 Geometries

Given that both horizontal encounters and encounters where the intruder is approaching from above and below are possible, the sUAS DAA test encounter geometry set should include both horizontal encounters and encounters that include vertical closure. For these tests, horizontal encounter angles are (clockwise) relative inbound course angles of the MA relative to the sUAS direction of travel as related to the Encounter Focal Point (EFP) as illustrated in Fig 1a. Thus, a horizontal angle of 0° is from the direction of sUAS track/heading (head-on). Vertical angles are elevations relative to the horizontal plane with the EFP as the reference point (Figure 1b).³

During the September 2020 tests, horizontal encounters were executed. Because a Ground Based Detect And Avoid (GBDAA) system that has no horizontal Field of View (FoV) limitations was utilized, the full range of possible horizontal encounter angles (0° - 360°) were tested at 45° increments (0° , 45° , 90° , 135° , 180° , 225° , 270° , 315°).

In addition, collision trajectories, in which the two aircraft are initially heading at each other (with a vertical safety offset), were utilized. These were used because they result in the most strict timing requirements for DAA for each encounter angle.

Thus, the encounter geometries used in the September 2020 tests include horizontal direction variations (one of the four dimensions of variability). They do not include all possibilities for this dimension, however, as:

- They are straight-line encounters and thus do not involve any turns by either aircraft.
- They only include collision-type geometries (in the horizontal direction) and, thus, exclude encounters that would result in loss of well clear but not a collision (non-collision geometries).

2.1.2.2 Speed Variations

Horizontal speed variations were included in the September 2020 tests. For these tests, speed variations were incorporated by altering the inbound speed of the intruder. Two speeds, 80 kts and 100 kts, were used. All possibilities for variation of this dimension are not included, however, as accelerations for either aircraft while inbound to the EFP were not included in the test design.

³ It is noted that these are not the same as relative bearing, which is the angle measured clockwise from the heading of the UA to the location of the intruder, with the UA being the anchor point.

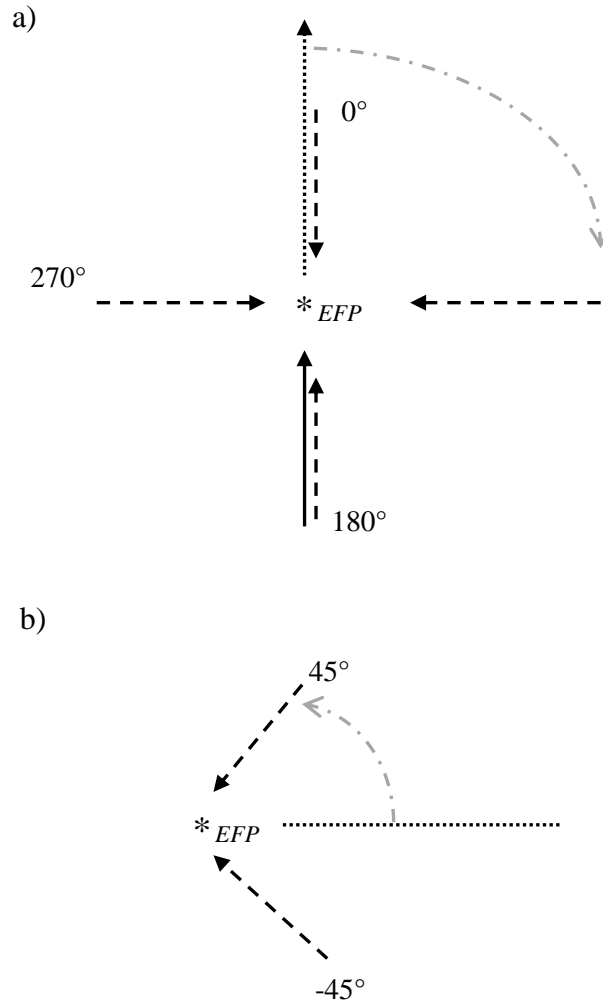


Figure 1. Illustration of encounter geometry angles in the horizontal and vertical planes. In a), the solid arrow indicates the flight path/course of the UA (Unmanned Aircraft); dashed arrows indicate intruder flight paths/courses projected onto the horizontal plane, the dotted line indicates the reference for horizontal encounter angles, and the gray dash-dot line indicates the angle for the 90° horizontal encounter angle. In b), the flight path/course of the UA is into the page, dashed arrows indicate intruder flight paths/courses, the dotted line indicates the reference for vertical encounter angles, the gray dash-dot line indicates the angle for the 45° vertical encounter angle, and the intruder is assumed to approach the EFP from a 90° horizontal encounter angle for ease of illustration.

2.1.2.3 Considerations for LR

The September 2020 tests included the following variations:

- Horizontal direction variations
- Horizontal speed variations

Variations that are not included are:

- Horizontal direction variations associated with:
 - Turns by either aircraft
 - Non-collision geometries
- Horizontal speed variations associated with:
 - Accelerations by either aircraft
- Vertical direction
- Vertical speed/rate

It is noted that this list of unincluded variations is subject to the following caveats:

- Maintaining a perfect heading while inbound to the EFP is not possible for either aircraft. These slight variations in heading had no discernable impact on the tests as they had no apparent effect on identification of conflicts or on maneuvers.
- Establishing perfect timing such that both aircraft would arrive at the EFP at the same time is not possible. Consequently, the encounters were not perfect collision geometries.
- Maintenance of a constant speed while inbound to the EFP is not possible for either aircraft. Beyond potential impacts on the collision geometry (i.e., altering from a collision-geometry to a non-collision geometry), no impacts owing to these slight changes in horizontal speed were identified.
- Maintenance of constant altitude while inbound to the EFP is not possible for either aircraft. Observed variations in vertical direction and vertical speeds/rates had no discernable impact on identification of conflicts or on maneuvers.

Use of data from these tests results in LR (well clear risk ratio) values that are different from those obtained by including all types of encounters. Use of only horizontal encounters is expected to have a relatively small impact on risk ratio values, for instance, as climb/descent encounters—especially those associated with crop sprayers that pop-up with limited time to respond—are expected to be challenging for DAA systems, but rare with adequate route planning. On the other hand, use of collision geometries is expected to generally produce larger LR values because they create the most strict timing requirements for each encounter angle. Hence, if LR values are estimated from collision geometries then in general it may be expected that the values are larger than if they were estimated through a random distribution of encounter geometries. Exceptions occur when sensors used have poor track accuracy and any maneuver helps to prevent a collision when aircraft are on collision geometries. This approach only works when there is sufficient track accuracy to know how to maneuver with respect to an intruder and the maneuver strategy actually attempts to increase separation in contrast to strategies that hover or hold. Other factors that impact LR values include use of linear trajectories (as opposed to curved trajectories for ownship and/or the intruder) and of constant horizontal speed trajectories. Because of these considerations, LR values herein are labelled with the symbol LR_{ch} , where the ‘c’ stands for collision (geometry) and the ‘h’ indicates horizontal encounters.

An additional important consideration is the limited number of samples that can be collected during flight testing. Risk ratios are commonly evaluated using a very large number (1000s or more) of simulations (e.g., ICAO 2014, §4.4.2.6; Deaton and Hansman 2019). In contrast, a week of flight testing will produce on the order of 100 encounters. Consequently, the risk ratio estimates obtained from flight tests have more sample uncertainty than do those from simulations. For this

reason, risk ratio estimates obtained through flight testing are referred to herein as sample risk ratios.

2.2 Test Objectives

The objectives of the September 2020 flight tests were:

- Collection of enough data to estimate LR_{ch}
- Determination if the test methodology allows for maintenance of well clear during encounters
- Determination if the test methodology supports proper testing of the DAA system

2.3 Test Personnel

Test partners are provided in Table 3. The UND and NPUASTS have been working with L3Harris™ Technologies for years and have developed a terrestrial UAS BVLOS capability that utilizes a C-Speed LightWave radar, Surveillance and Broadcast Services (SBS) ADS-B data, and Xtend™ ADS-B (L3Harris 2021) data. The L3Harris™ system includes visualization through the L3Harris™ RangeVue™ (Harris 2016) product as well as an alerting and guidance system to warn of potential conflicts. A combination of these systems was used in the September 2020 tests.

Table 3. UND-NPUASTS September 2020 test partners.

Partner	Role
NPUASTS	Flight Test Coordinator, Technology Provider
UND	Project Coordination, Manned Aircraft Intruder, Technology Provider
SkySkopes	UAS Operator
L3Harris™	Technology Provider

2.3.1 NPUASTS

The NPUASTS provided the Flight Test Director (FTD), who was based in the NPUASTS Operations Trailer, which was parked at the Lovas Farm (cf. §2.6). The FTD was the primary person leading the execution of the flight tests and oversaw operations using multiple data feeds and communicated directly with the flight teams via Stonecast radios, which utilize a radio tower network in northeast North Dakota (Stones Mobile Radio 2021). The NPUASTS provided Mission Commanders (MCs) to assist and ensure that flights adhere to NPUASTS Standards and Policy. The NPUASTS also provided data collectors and visual observers. The NPUASTS provided a suite of visualization, DAA, and data collection technologies in concert with the technology-providing partners on this project.

2.3.2 UND

The UND provided the data collection and analysis team, Principal Investigator (PI), intruder aircraft (Cessna 150), and FAA (Federal Aviation Administration) and press interface personnel.

The PI interfaced with the FTD to ensure all goals were accomplished for the test event. It is noted that Mr. Stephen Luxion from Mississippi State University ASSURE Management (MSU - ASSURE) supported the September 2020 tests by acting as a conduit to the FAA.

2.3.3 SkySkopes (UAS Operator)

SkySkopes flew the Robot Aviation FX20 UAS. SkySkopes provided a flight crew (2-3 people), flight system, and spare batteries and parts.

2.3.4 L3 Harris Technologies

L3Harris™ provided a suite of GBDAA technology and UAS network infrastructure to support BVLOS operations. L3Harris™ collaborated with SkySkopes to integrate a data feed from the FX20 UA GCS (Ground Control Station) into the L3Harris™ DAA system at Hillsboro, ND, to provide ownership data to the L3Harris™ system. L3Harris™ also provided remote support for the system (including data collection).

2.3.5 Distribution and Roles

Personnel distribution, systems, and data sources for the core capabilities applied during the September 2020 tests are illustrated in Figure 2. The three primary operational locations were the Command Center Trailer, the Electronic Observer Trailer, and the UA LRE (Launch and Recovery Element). Each of these were at different locations: the Command Center Trailer was at the Lovas farm, the Electronic Observer Trailer was at the Hillsboro, ND, airport (co-located with the C speed radar), and the UA LRE was either at the Lovas farm or just across the coulee that passes south of the Lovas farm. More information regarding locations is provided in the Test Locations section.

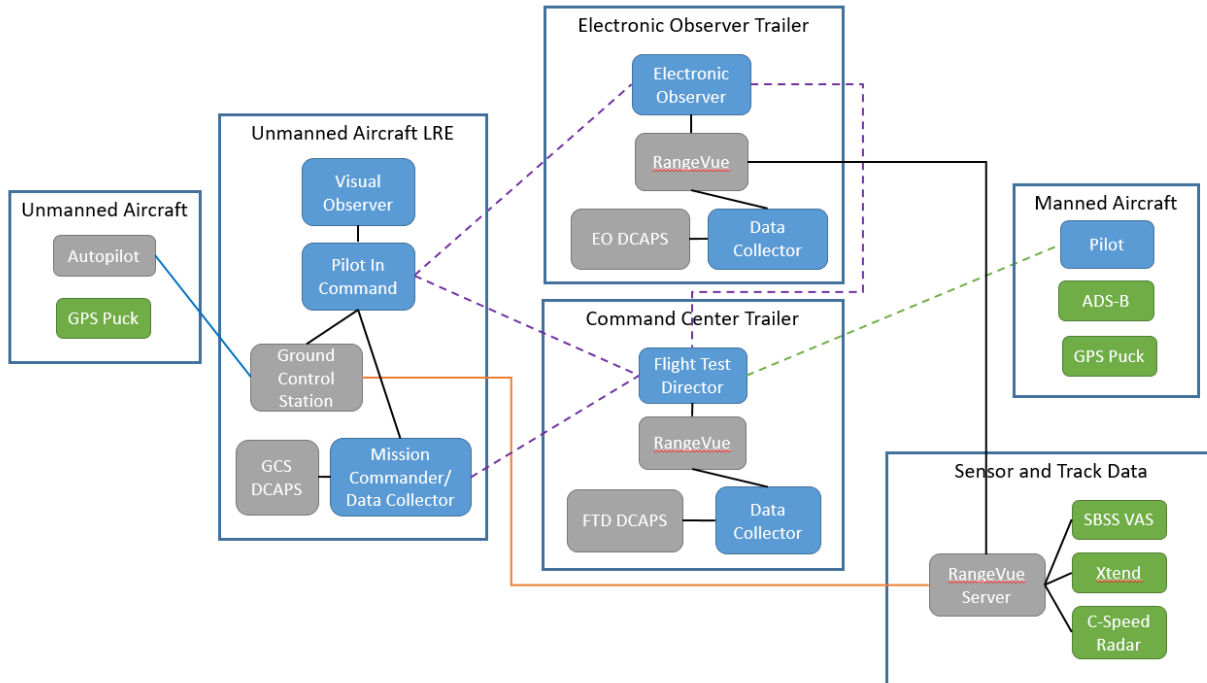


Figure 2. Personnel distribution, systems, and data sources for core September 2020 flight test capabilities. Personnel roles are shaded blue, systems are shaded grey, and data sources are shaded green. Communications/connections are indicated with lines, with solid black indicating a direct/wired connection, solid blue indicating the GCS-UA connection, solid orange indicating communication via LTE (Long-Term Evolution), dashed green indicating communications with the manned aircraft via VHF (Very High Frequency) radios, and dashed purple indicating communications via Stonecast radios.

As indicated in Figure 2, data flow into the L3Harris™ system through what is labelled as “RangeVue Server”. Details regarding this architecture are beyond the scope of this document. However, it is noted that multiple servers were being utilized, with the EO RangeVue™ system receiving UA telemetry via LTE (Long-Term Evolution) to enable the EO to perform its functions and to feed A&G (Alerting and Guidance). The RangeVue™ server acquires cooperative data from the L3Harris™ SBSS (Surveillance and Broadcast Services Subsystem) VAS (Value Added Service) and from local Xtend™ ADS-B units (L3Harris 2021). For the September 2020 tests, the RangeVue™ server collected noncooperative data from a C Speed Lightwave Radar (C Speed 2021). In addition, GPS (Global Positioning System) pucks, which are portable, self-powered GPS systems were utilized to collect truth data for aircraft position. The same type of GPS unit was used on both the unmanned and MA. An additional source of truth data for aircraft position is the ADS-B unit onboard the MA.

Systems illustrated in Figure 2 are:

- Command Center Trailer
 - RangeVue™: L3Harris™ DAA display system
 - Flight Test Director DCAPS (Data Collection And Processing System): A system that enables collection of DAA test data (described further in the Data Management section)
- Electronic Observer Trailer

- RangeVue™: L3Harris™ DAA display system
- Electronic Observer DCAPS: A system that enables collection of DAA test data
- Unmanned Aircraft LRE
 - Ground Control Station: FX20 GCS
 - Ground Control Station DCAPS: A system that enables collection of DAA test data
- Unmanned Aircraft
 - Autopilot: The FX20 autopilot
- Sensor and Track Data
 - RangeVue™ server: System that collects cooperative and noncooperative data and provides those to systems/displays.

Additional systems (beyond those illustrated in Figure 2) were utilized during the tests, including:

- Computers and network infrastructure: Throughout the system
- Xtend™ ADS-B: An Xtend™ unit was also utilized at the Command Center Trailer
- Weather Station: Used to monitor winds, etc., at the Command Center Trailer
- Simulyze: A data fusion and display system utilized by the NPUASTS
- Stratus 2 and SkyRadar DX: ADS-B units that provide data to Simulyze
- DVR (Digital Video Recorder) and Cameras: Video collection system in the Command Center Trailer for capturing operations (can capture video from both inside and outside of the trailer).

Communications were accomplished in several ways:

- Direct/Wired: Either direct (e.g., viewing a screen) or wired connections (solid black lines in Figure 2)
- Radio link for FX20 GCS-UA (solid blue line in Figure 2)
- LTE (solid orange line in Figure 2)
- VHF for FTD to manned aircraft (dashed green line in Figure 2)
- Stonecast radios (dashed purple lines in Figure 2)

The roles illustrated in Figure 2 are:

- Command Center Trailer
 - Flight Test Director (FTD; NPUASTS): Primary person leading execution of the flight tests
 - Data Collector (NPUASTS): One data collector utilized the FTD DCAPS to collect flight test data. Another data collector recorded metadata (manual notes).
- Electronic Observer Trailer
 - Electronic Observer (NPUASTS): Monitored RangeVue™ display and communicated maneuvers to UA PIC (Pilot in Command).
 - Data Collector (UND): Utilized the EO DCAPS to collect flight test data.
- Unmanned Aircraft LRE
 - Visual Observer (SkySkopes): Assists the PIC with see and avoid function
 - PIC (SkySkopes): Person with final authority and responsibility for operation and safety of the UA

- Mission Commander/Data Collector (NPUASTS): One person fulfilled this dual role of ensuring that flights adhered to NPUASTS Standards and Policy and utilizing the GCS DCAPS to collect flight test data.
- Manned Aircraft
 - Pilot (UND): Operated the manned aircraft

A high level overview of the testing process is provided in Appendix A and illustrated in Figure A1. Example test cards for scenario HE_0__100 (Horizontal Encounter with a 0° encounter angle and 100 kt intruder speed) are provided in Appendix B. As shown in these cards, the sequence of events is summarized as:

- The MA and UA move to their stand-off (starting) locations
- The MA starts inbound to the HEFP (Horizontal Encounter Focal Point)
- The FTD director directs the UA to begin its inbound leg to the HEFP
- Events such as first detection, track initiation, etc., are recorded
- The EO determines if a conflict exists
- If the EO determines a conflict exists, the EO identifies and maneuver and instructs the PIC to maneuver
- The FTD declares end of encounter

Additional types of data (e.g., time of closest point of approach) are collected by data collectors. The FTD coordinates events such as UA and MA launch and recovery.

2.4 DAA System

Testing was conducted using the L3Harris™ Technologies DAA system, which enables multiple approaches for the Evaluate component of DAA.⁴ Table 4 provides information regarding the L3Harris™ DAA System and regarding the two options for the Evaluate step.

⁴ In the related research effort that preceded this effort, Askelson et al. (2017) identified the major steps in DAA as Detect, Track, Evaluate, and Maneuver (DTEM). These are defined as Detect—sense the presence of something that must be avoided through some means; Track—estimate the path of the intruder; Evaluate—determine whether identified intruders pose a threat, prioritize threats, and identify maneuver; Maneuver—execute maneuver. These map to the functions in ASTM (2020) according to: Detect Function DF (Detect and Track), Alert Function A1F (portion of Evaluate wherein hazards are identified and prioritized), and Avoid Function A2F (portion of Evaluate where the maneuver is identified and Maneuver).

Table 4. Information regarding the L3Harris™ DAA system.

DAA Step	DAA Steps	Description
Detect	C-Speed Lightwave Radar and ADS-B (SBSS VAS and Xtend)	Detect data for non-cooperative targets are provided using a C Speed Lightwave Radar. Data for cooperative targets are provided through the SBSS (Surveillance and Broadcast Services Subsystem) VAS (Value Added Service) and through Xtend ADS-B units.
Track	Best-source selection	Data having the most accurate information regarding intruder locations/tracks are used. Track data are provided through the SBSS VAS or by the C-Speed Lightwave Radar.
Evaluate	EO (Electronic Observer) -or- Alerting and Guidance (A&G) supporting the EO	Either the EO performs all functions in this step or A&G is utilized to help the EO decide upon the maneuver. The display system is RangeVue™ and ownship data are ingested into the system through a telemetry feed from the UAS GCS.
Maneuver	Human Pilot	The FX20 flight crew executed maneuvers once received from the EO. This involved setting new waypoints for the FX20.

The L3Harris™ Technologies DAA system obtains intruder detection data from several sources. Non-cooperative data are provided using a C Speed Lightwave Radar (C Speed 2021; Figure 3). This is a low-cost, flexible, “software-defined”, S-Band, 2D (two-dimensional) radar technology platform that can serve a broad range of surveillance missions through reconfiguring of its run-time parameters. Cooperative data are obtained from the L3Harris™ SBSS (Surveillance and Broadcast Services Subsystem) VAS (Value Added Service) and from local Xtend™ ADS-B units (L3Harris 2021) that act as gap-fillers to provide surveillance coverage in areas that may not be effectively covered by the FAA’s system (provided through the SBSS VAS).



Figure 3. The C Speed Lightwave Radar utilized during the September 2020 flight tests.

Track data are provided by the L3Harris™ SBSS VAS (cooperative intruders) and the C Speed Lightwave Radar system. The L3Harris™ system performs a best source selection. Thus, it selects the surveillance source that provides the best information regarding an intruder and displays those data (locations and tracks). Generally, the source that provides the lowest uncertainty regarding intruder location is considered to be the best source. Thus, these flight tests generally utilized a cooperative DAA system. This, however, had no deleterious impact on test objectives.

As indicated in Table 4, the L3Harris™ system can be used two different ways for the Evaluate step. For the September 2020 flight tests, the A&G capability was not utilized because guidance was not generally provided. This presumably occurred because of the availability of ADS-B surveillance data for the intruder. With those data, the A&G likely recognized the vertical offset between the aircraft (nominally 350 ft).⁵ The A&G system is still being developed, however, and thus the lack of guidance could have occurred for other reasons. Consequently, the EO used the RangeVue™ display to identify conflicts and determine maneuvers. The EO used a Stonecast radio to communicate maneuvers to the UA PIC.

Maneuvers were executed by the UA PIC. Callbacks of commanded maneuvers were commonly used for acknowledgement.

⁵ A 350 ft vertical offset was utilized to enhance safety.

2.5 Test Aircraft

The UA (Unmanned Aircraft) that was flown is SkySkopes' FX20 UAS manufactured by Robot Aviation. Specifications for the FX20 are provided in Table 5.

The C150 intruder aircraft is owned by UND and was operated by UND during the September 2020 flight tests. Information regarding this aircraft is provided in Table 6.

Table 5. Information regarding the UA used during the September 2020 flight tests.



		The FX20 is a high-performance medium-range UAS that can be operated by a crew of two and transported in a small truck or van. Its design results in extremely low energy consumption. As a result, the all-electric flying wing can stay in the air for multiple hours (approaching 4 hrs). A portable launcher allows for runway-independent operation, with recovery conducted using either a net or skids.	
Wing Span	3.0 m	Cruise Speed	27 m s ⁻¹
Maximum Takeoff Weight	12 kg	UAS Operator	SkySkopes
Endurance	2 hr	GCS Type	Robot Aviation
Autopilot	Micropilot		

Table 6. Information regarding the intruder aircraft used during the September 2020 flight tests.

		The Cessna 150 is a two-seat, tricycle-gear general aviation airplane that was designed for flight training, touring, and personal use.	
Wing Span	33 ft 2 in	Cruise Speed	82 kts
Maximum Takeoff Weight	1,600 lb	Operator	UND
Fuel Capacity	22.5 US gal		

2.6 Test Locations

2.6.1 Locations of Test Elements

The Command Center Trailer illustrated in Figure 2 was located at the Lovas Farm, at approximately (-97.082223, 47.329763). One UA LRE was at approximately (-97.084370, 47.329733), which is at the Lovas Farm and very near the Command Center Trailer, and the other UA LRE was at approximately (-97.090454, 47.327013). The DAA system, C Speed radar, and Electronic Observer Trailer were located on the ramp of the Hillsboro, ND, airport at (-97.061847, 47.357982). The Hillsboro airport is approximately 1.8 nm northeast of the Lovas Farm. For

reference, the HEFP was at (-97.087696, 47.328505). The locations of the Command Center Trailer, one UA LRE, and the Electronic Observer Trailer are illustrated in Figure 4.

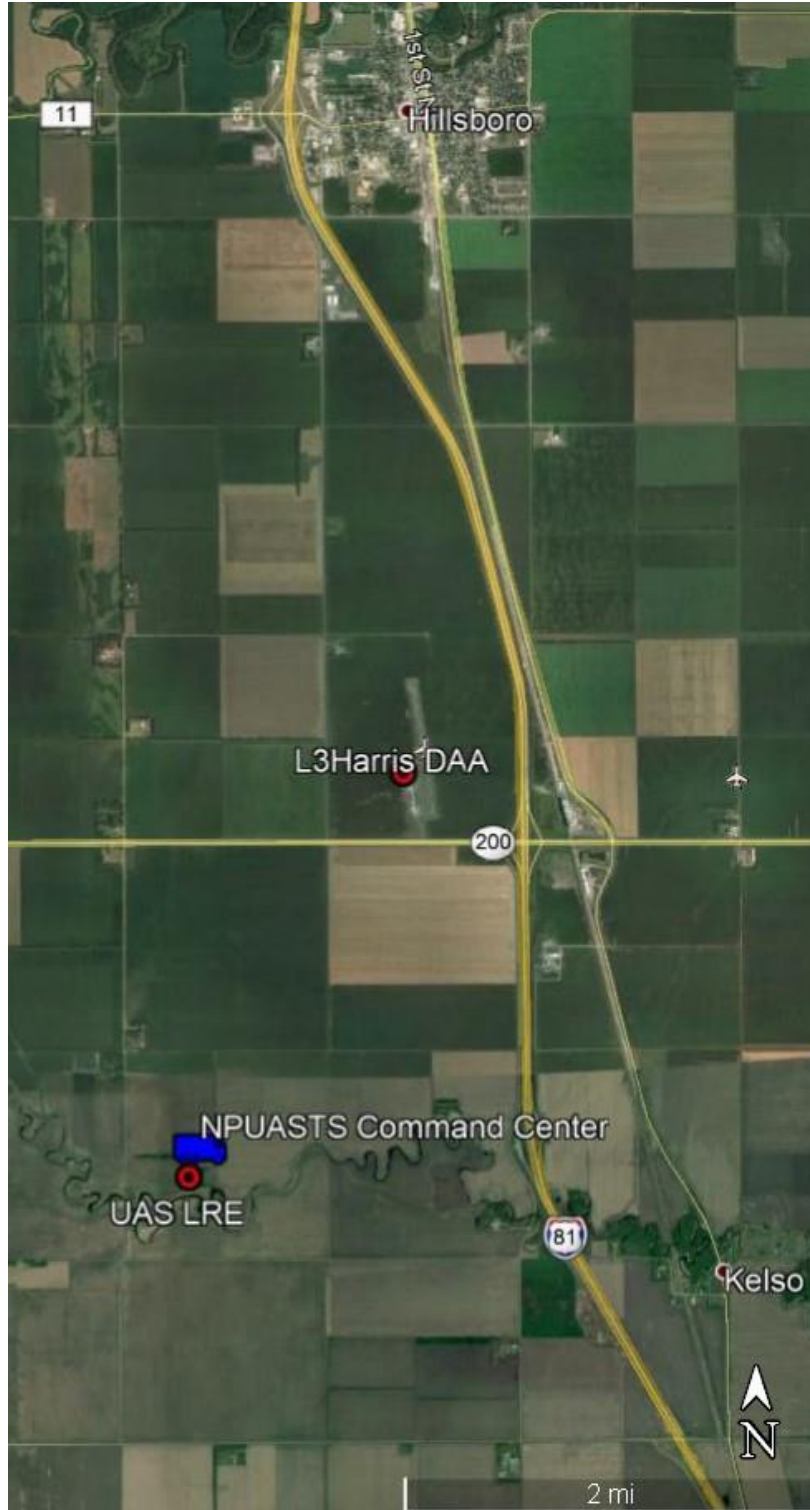


Figure 4. Locations of testing elements during the September 2020 flight tests.

The UA was flown to the southwest of the Hillsboro airport to avoid any issues with the airport. The manned aircraft launched from the Grand Forks International Airport (KGFK) and refueled at the Hillsboro Airport (3H4) as needed. Figure 5 provides a sectional for the area. The test area is Class G airspace up to 700 ft AGL (Above Ground Level) and Class E airspace above 700 ft AGL (up to Class A airspace).



Figure 5. Sectional centered on the September 2020 flight test area.

Figure 6 provides images from the Lovas Farm, the location of the Command Center Trailer and one UA LRE. That UA LRE was approximately in the location of the large snowbank near the barn shown in the upper-right panel of Figure 6. Flights tests were conducted to the south and west of the Lovas Farm.



Figure 6. Images from the Lovas farm, the location of the Command Center Trailer and one UAS LRE. View is to the north (upper-left), to the east (upper right), to the south (lower left), and to the west (lower right).

2.6.2 Georeferenced Encounter Geometry Generation

The eight horizontal encounter angle geometries were generated by having the MA fly the same path either northwest to southeast or southeast to northwest and by varying the UA origination point. The two scenarios for MA flight direction are illustrated in Figures 7 and 8. The encounter geometries associated with UA origination points for the MA flying northwest to southeast (Figure 7) are:

- A. 0°
- B. 315°
- C. 270°
- D. 225°
- E. 180°

The encounter geometries associated with UA origination points for the MA flying southeast to northwest (Figure 8) are:

- B. 135°
- C. 90°
- D. 45°

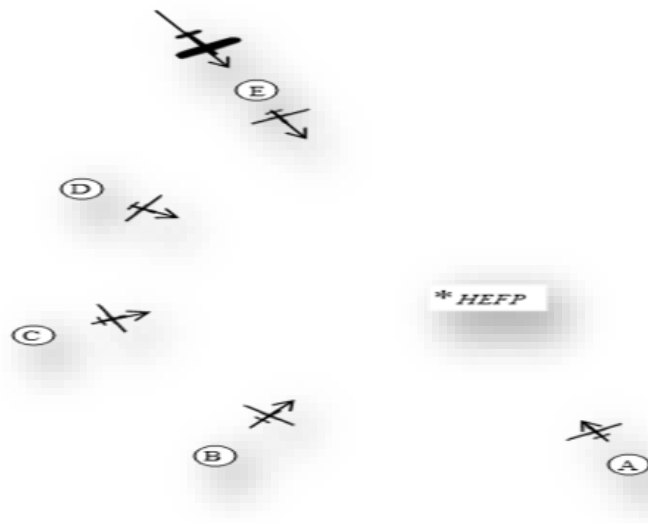
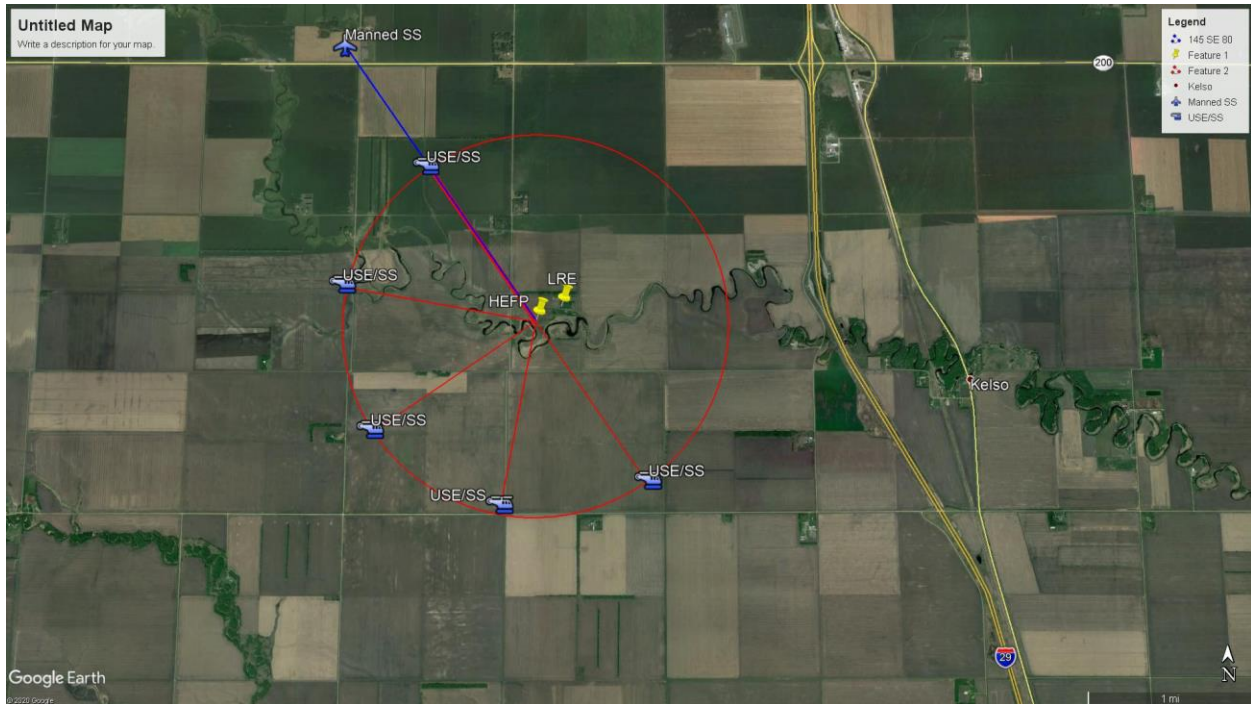


Figure 7. Illustration of encounters associated with the MA flying northwest to southeast. The top image illustrates aircraft paths and origination points. The bottom figure provides labels for UA origination points.

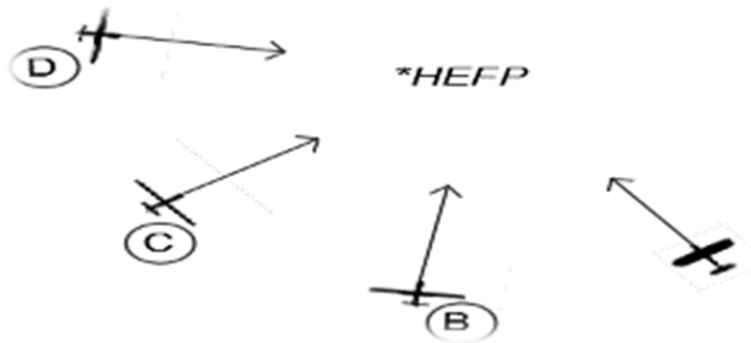
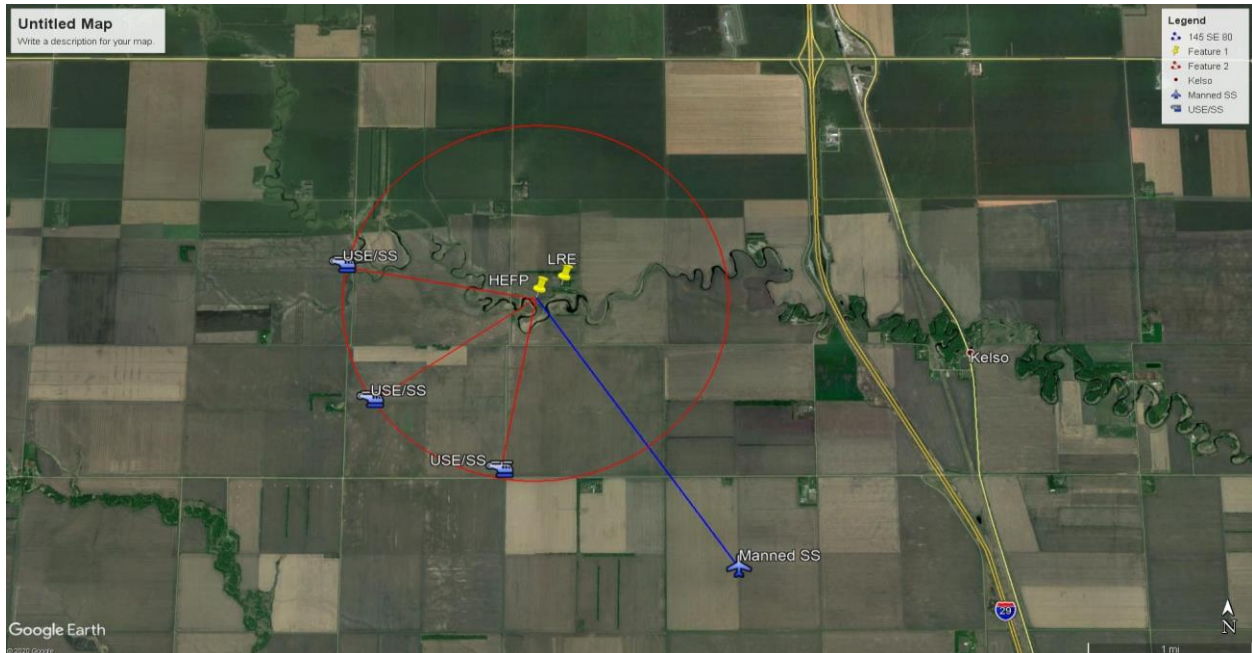


Figure 8. As in Figure 7 but for the MA flying southeast to northwest.

2.7 Test Dates and Schedule

Tests were conducted during the week of 20-26 September 2020. 21 September 2020 was a shakedown day, with flights planned for the afternoon if possible. The primary flight tests days were 22-25 September 2020. The schedule for a nominal test day is provided in Figure 9.

Start	End	Day 1 (September 21, 2020)	Day 2 (September 22, 2020)	Day 3 (September 24, 2020)	Day 4 (September 25, 2020)	Day 5 (September 26, 2020)
0600	0630					Weather Day
0630	0700					
0700	0730	Meet at NPUASTS (4201 James Ray Drive)	Meet at NPUASTS (4201 James Ray Drive)	Meet at NPUASTS (4201 James Ray Drive)	Meet at NPUASTS (4201 James Ray Drive)	
0730	0800	Travel to Site	Travel to Site	Travel to Site	Travel to Site	
0800	0830	Morning Briefing	Morning Briefing	Morning Briefing	Morning Briefing	
0830	0900	Site Setup and Preparation	Site Setup and Preparation	Site Setup and Preparation	Site Setup and Preparation	
0900	0930					
0930	1000					
1000	1030					
1030	1100	Flight Testing	Flight Testing	Flight Testing	Flight Testing	
1100	1130					
1130	1200					
1200	1230	Lunch and Aircraft refueling	Lunch and Aircraft refueling	Lunch and Aircraft refueling	Lunch and Aircraft refueling	
1230	1300					
1300	1330					
1330	1400					
1400	1430	Flight Testing	Flight Testing	Flight Testing	Flight Testing	
1430	1500					
1500	1530					
1530	1600					
1600	1630	Site and Equipment tear down	Site and Equipment tear down	Site and Equipment tear down	Site and Equipment tear down	
1630	1700					
1700	1730	Debrief and schedule review	Debrief and schedule review	Debrief and schedule review	Debrief and schedule review	
1730	1800					
1800	1830	Travel to NPUASTS	Travel to NPUASTS	Travel to NPUASTS	Travel to NPUASTS	

Figure 9. Schedule for a nominal test day.

2.8 Test Conditions

Weather conditions for flight tests conform to Part 107 requirements (e-CFR 2021b) since the FX20 was operated under Part 107. No notable challenges regarding electromagnetic interference were identified prior to or during testing.

2.9 Test Cards

Test cards were developed for three roles: FTD, UA pilot, and MA pilot. A total of 48 cards (8 encounter angles x 2 intruder speeds x 3 roles) supported this test campaign. Example test cards are provided in Appendix B. In addition to a change in desired intruder speed, values that changed in test cards are associated with the origination points of the UA and MA. The origination points for the UA and MA are provided in Table 7. UA origination points having the same letter identifier are the same for the 80 kt and 100 kt encounters because the desired speed of the UA did not vary.

Table 7. Origination points for the UA and MA used during the September 2020 flight tests.

Aircraft	Speed	Origination Point	Longitude (°)	Latitude (°)
Manned	80	NW	-97.114674°	47.353510
Manned	80	SE	-97.060923	47.301665
Manned	100	NW	-97.121141	47.359589
Manned	100	SE	-97.054307	47.294743
Unmanned	80	A	-97.072817	47.312755
Unmanned	80	B	-97.092211	47.310628
Unmanned	80	C	-97.109559	47.317319
Unmanned	80	D	-97.113895	47.330578
Unmanned	80	E	-97.102953	47.341706
Unmanned	100	A	-97.072817	47.312755
Unmanned	100	B	-97.092211	47.310628
Unmanned	100	C	-97.109559	47.317319
Unmanned	100	D	-97.113895	47.330578
Unmanned	100	E	-97.102953	47.341706

Test cards were reviewed by the UND/NPUASTS team, the broader A18 team, and the FAA prior to execution. A key to ensuring safety was use of a 350 ft vertical aircraft offset during the execution of these horizontal (type) encounters.

2.10 Data Collection and Management

2.10.1 Metadata

Metadata regarding the executed tests were collected. These data were generally collected using a spreadsheet like that illustrated in Figure 10. Metadata were also collected by various participants in the form of hand-written notes. These include notes collected by the FTD and by the data collector in the Electronic Observer Trailer.

COMPLETION RATING												
General Day/Site Information												
DATE	LOCATION ID	EVENT ID	TIME	INITIAL_WX_CONDITIONS	EQUIPMENT_NOTES	SCHEDULE_ADJUSTMENTS_MADE						
Test Scenario Static Information												
SCENARIO #	EVENT ID	SCENARIO_START_TIME	SCENARIO_END_TIME	UAS_MAKE/MODEL	INTRUDER_MAKE/MODEL	FAA_RULE	WAIVER/COA #	VLOS/EVLOS/BVLOS	OOB			
Encounter Specific Information												
SCENARIO #	COMPLETION RATING	EVENT ID	TEST CARD	TRIAL #	UAS_LAUNCH_TIME	UAS_RECOVERY_TIME	INTRUDER_LAUNCH_TIME	INTRUDER_RECOVERY_TIME	UAS_ALTITUDE	INTRUDER_ALTITUDE	UAS_SPEED	INTR

Figure 10. Spreadsheet utilized to capture test metadata.

2.10.2 DCAPS

The Data Collection And Processing System (DCAPS) was used to collect data regarding events that occurred during testing. DCAPS was developed by an L3Harris™ partner during previous research projects and provides a very convenient means for collecting DAA test data. Within DCAPS, different roles (e.g., data collector at the Electronic Observer Trailer) with associated events are defined. These events are presented as buttons. Selection of these events/buttons results in recording of the event time, time, and origination station for that record. Numerous DCAPS stations can be active during a test, with the data stored in a combined file. In addition, comments can be added by users to collect notes. DCAPS interfaces for the GCS, EO, and FTD are shown in Figures 11-13.

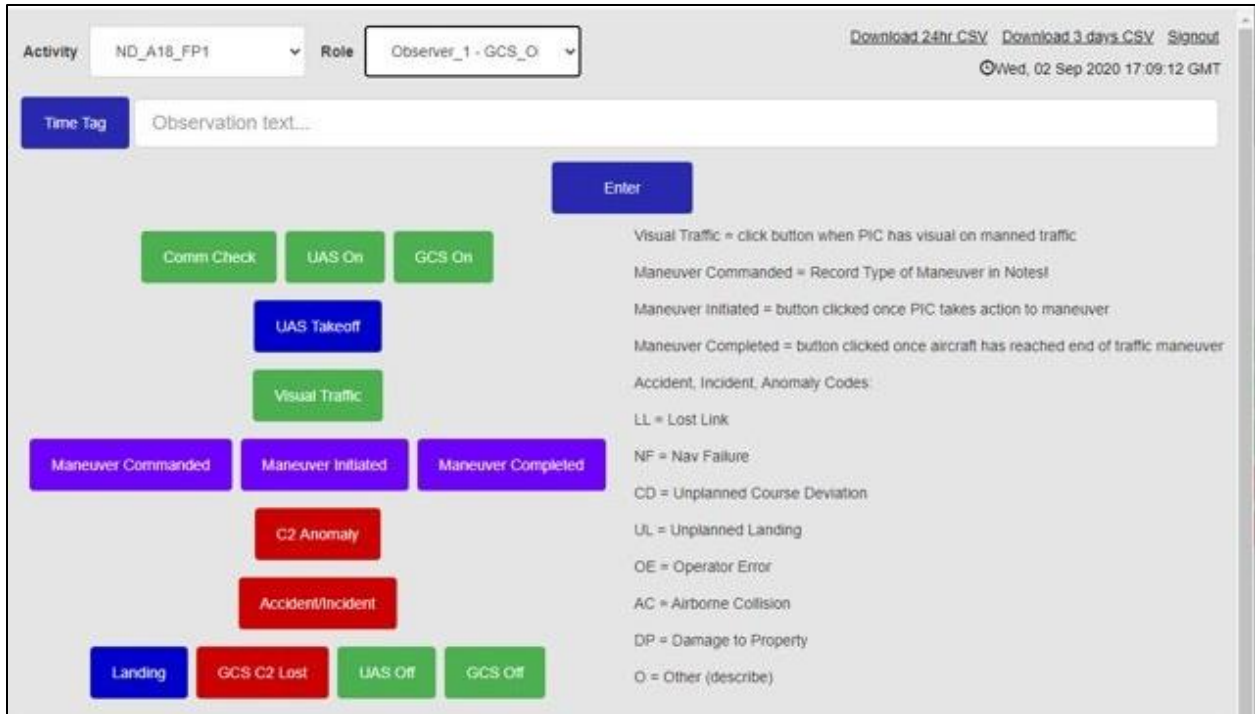


Figure 11. GCS DCAPS interface.

The interface displays a top navigation bar with 'Activity' set to 'ND_A18_FP1' and 'Role' set to 'EO1 - EO_Observer'. It includes links for 'Download 24hr CSV', 'Download 3 days CSV', and 'Signout', along with a timestamp 'Wed, 02 Sep 2020 17:07:59 GMT'. Below this is a 'Time Tag' field with 'Observation text...' and an 'Enter' button.

The main area contains a grid of buttons for recording events:

- Comm Check (Green)
- Area Clear (Blue)
- EO's Responsibility (Blue)
- First Detection (Green)
- Track Established (Green)
- Maneuver Start Displayed (Purple)
- Maneuver Stop Displayed (Purple)
- CPA (Blue)
- Traffic Advisory (Yellow)
- Traffic Update (Blue)
- Traffic Alert (Orange)
- Traffic Warning (Dark Red)
- Traffic No Factor (Blue)
- WC Violation (Red)
- WC Regained (Red)
- Surveillance anomaly (Red)

On the right side, a list of definitions is provided:

- First Detection = click button when sensor first detects intruder
- Track Established = click button when system creates track
- Maneuver Start Displayed = click button once EO sees UAS start maneuver
- Record Maneuver Type Observed (climb, descend, turn) in Notes!
- Maneuver Stop Displayed = click button when EO thinks end of maneuver was reached
- CPA = click button when EO thinks closest CPA occurs
- Traffic Advisory = click button when a traffic advisory is issued
- Traffic Update = click button when a traffic advisory is updated
- Traffic Alert = click button when a traffic alert is issued
- Traffic Warning = click button when a traffic warning is issued
- Traffic No Factor = click button when a traffic call is considered no-factor
- Surveillance Anomaly = click button and record notes if surveillance issue is seen

Figure 12. EO DCAPS interface.

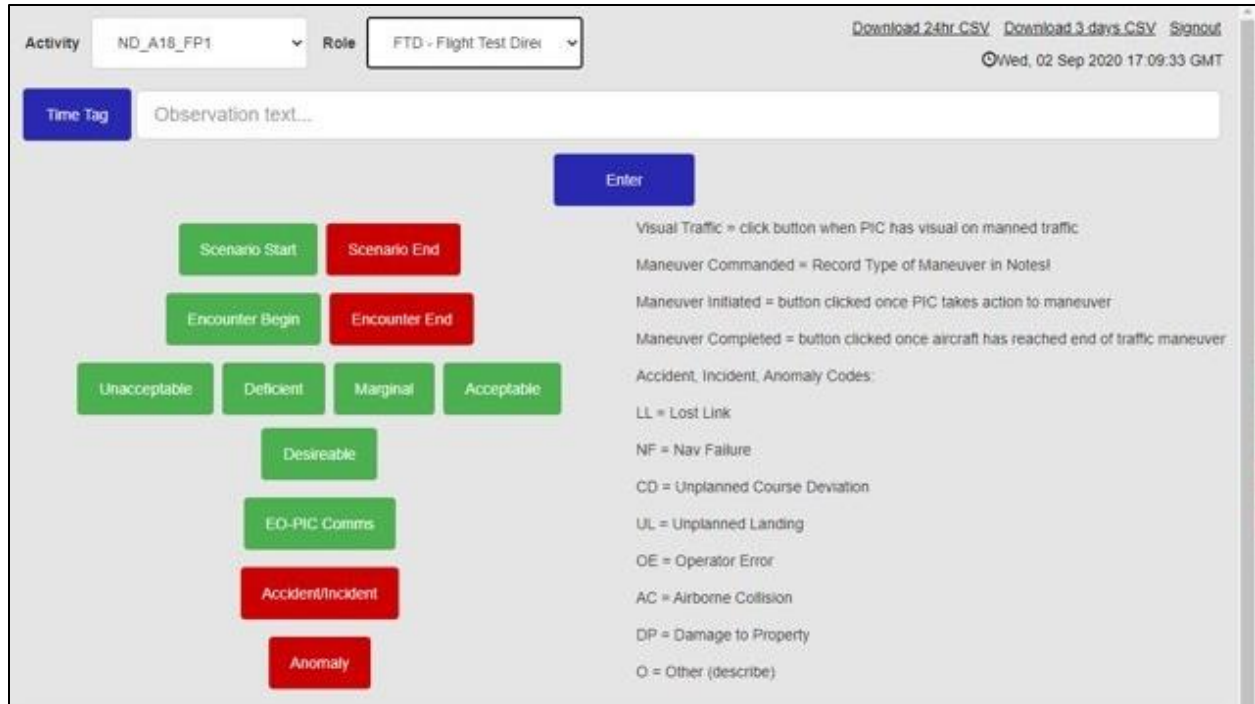


Figure 13. FTD DCAPS interface.

2.10.3 Aircraft Position Truth Data

For both the UA and MA, aircraft position data were collected using Qstarz BT-Q1000XT GPS pucks (Qstarz 2021). These self-powered pucks are very easy to use, being activated with a single switch. The data are, by default, enhanced by the Wide Area Augmentation System (WAAS) (USDOT 2021). This system improves location accuracy by decreasing horizontal and vertical position errors to roughly 1/2 and 1/4 of those produced by Standard Positioning Services (SPSs), respectively. As indicated in Table 8, errors for Minneapolis, which is the closest station provided by FAA William J. Hughes Technical Center (2020), are less than 1 m in both the horizontal and vertical directions 95% of the time, indicating that the aircraft position truth data utilized in these tests are expected to be highly accurate. The data from FAA William J. Hughes Technical Center (2020) are for the period 1 July – 30 September 2020.

Table 8. GPS errors from Table 2-1 of FAA William J. Hughes Technical Center (2020).

Location	WAAS 95% Horizontal (m)	WAAS 95% Vertical (m)	SPS 95% Horizontal (m)	SPS 95% Vertical (m)
Average of 38 Locations	0.63	1.04	1.59	3.6
Minneapolis	0.61	0.96	1.53	3.44

In addition to data collected with the Qstarz BT-Q1000XT GPS pucks, MA ADS-B data were also collected. These data supplemented the Qstarz BT-Q1000XT GPS data. The team attempted to acquire UA position data from the UAS Operator, but were unable to acquire those data owing to challenges the UAS Operator encountered with data recording.

2.10.4 Additional Data Sets

Additional data were collected during the test period. These include:

- C-Speed Lightwave Radar: Data from the C-Speed Lightwave Radar were collected and stored.
- RangeVue™: Data handled with the RangeVue™ system are logged by L3Harris™. This includes FAA ADS-B and radar data provided by SBSS VAS.
- Xtend™ ADS-B: An Xtend™ unit was also utilized at the Command Center Trailer.
- Stratus 2 and SkyRadar DX: ADS-B units that provide data to Simulyze.
- Weather Station: Used to monitor winds, etc., at the Command Center Trailer.
- DVR and cameras: Video collection system in the Command Center Trailer for capturing operations (can capture video from both inside and outside of the trailer).

3 DATA ANALYSIS

3.1 Metrics

Results from this set of flight tests are organized according to individual encounters and the overall test campaign.

3.1.1 Individual Encounter Metrics

3.1.1.1 Encounter Events

Encounter events that are captured are related to well clear status. These are:

- Well clear violation
- Horizontal well clear violation
- Vertical well clear violation

Well-clear violations occur when the vertical aircraft safety offset failed to maintain vertical well clear status and the DAA operation failed to maintain horizontal well clear status. A horizontal well clear violation occurs for these horizontal (type) encounters when the DAA operation failed to maintain horizontal well clear status and the vertical aircraft safety offset enabled maintenance of vertical well clear status. A vertical well clear violation occurs when horizontal well clear is maintained but vertical well clear is not maintained.

Tracking vertical well clear violations assists with evaluation of the efficacy of the vertical aircraft safety offset. However, vertical well clear violations can happen during segments of encounters that are not relevant. This includes the beginning and end of encounters when aircraft may be maneuvering to set-up the next encounter, landing, etc. Thus, vertical well clear violations are only identified if they occur during the Objective Encounter Period (OEP), which is defined in the next section.

3.1.1.2 Encounter Descriptors

Qualities that define portions of the encounters are used to enable analysis. The first is the beginning and end of the inbound (to the HEFP) portions of flight paths for both aircraft. An aircraft is inbound (to the HEFP) when the following are realized:

- Projection of the position of the aircraft ahead, using its current heading, the distance it is from the HEFP is within a certain distance of the HEFP.
- Distance to the HEFP is decreasing.
- An aircraft is not maneuvering.

All of the encounters were examined to determine the tolerance distance relative to the HEFP (first condition above). A tolerance distance of 2500 ft was used. While aircraft generally would pass much closer to the HEFP if no maneuvering occurred, occasionally the MA would miss the HEFP by distances that approached $\frac{1}{2}$ of a mile.

The last criterion in the above list is whether the aircraft is maneuvering. Because the planned trajectories for the MA were straight, maneuvers were identified only for the UA. Maneuvering is identified from GPS puck data and stored using flags that indicate if the aircraft turned or climbed/descended. In addition to these, the type of turn or whether the aircraft was climbing/descending is indicated according to:

- Turn type:
 - R: Right
 - L: Left
- Climb/descent:
 - C: Climb
 - D: Descend

A three-dimensional maneuver involving both a turn and climb/descent can be identified using the combination of variables for turning and climb/descent. It is noted that the software does not currently properly label maneuvers in which an action is suspended (e.g., suspension of descent). Such maneuvers are identified, but are given a potentially-misleading label (suspension of descent, for instance, would be labelled as 'C').

Both turning and climb/descents are identified using differences between data that have been smoothed using a running average of length 3. Such smoothing was applied to eliminate false indications of turns or climbs/descents that arise owing to small-scale variations in aircraft position caused by turbulence, GPS errors, etc. Turns are identified when the current turn rate (after application of running average) differs from the previous turn rate at the previous GPS puck position (after application of running average) by 7 deg s^{-1} . This value was derived by examining turn rate differences during the OEP for all satisfactory encounters that were executed during this flight test campaign.

Climbs or descents are identified in a similar manner using differences in climb/descent rates for data smoothed using a running average of length 3. Currently, the threshold for identifying climbs/descents is 7 ft s^{-1} . ASTM (2020) states that a nominal climb/descent rate for when vertical direction indicators are needed for intruders is 8.33 ft s^{-1} . ASTM (2020) also states that a low UA vertical agility is associated with 4.167 ft s^{-1} and a high UA vertical agility is associated with 8.33 ft s^{-1} . It is noted that since these tests did not involve vertical maneuvers, data from these tests

were not useful for identifying vertical maneuver thresholds. Thus, the threshold used in the software may need to be modified for tests that involve vertical maneuvers.

The beginning of the UA maneuver period is identified by searching for a maneuver that occurs after the beginning of the inbound portion of the UA flight path. The end of the maneuver is defined, for horizontal (type) encounters, as:

- If a well clear or horizontal well clear violation occurred, the time when well clear or horizontal well clear was regained.
- If neither a well clear nor horizontal well clear violation occurred, the time when the horizontal distance between aircraft begins to increase.

Another important period during an encounter is the OEP. This is the period within an encounter when the two aircraft are deemed to be interacting and is, then, the relevant period of an encounter. It is defined by:

- Beginning: The earliest time when both aircraft are inbound to the HEFP.
- End: The earliest of either the declared end of encounter (from DCAPS data) or when the horizontal distance from the well clear boundary exceeds 2000 ft and the horizontal distance between aircraft is increasing with time.

The condition of being 2000 ft beyond the horizontal well clear boundary was chosen because at that distance the unmitigated NMAC risk is reduced to approximately half of its value that occurs at the horizontal well clear distance (Weinert et al. 2018).

3.1.1.3 Distance Metrics

One distance metric that is used is distance to the well clear volume, d_{wc} , which quantifies how near one came to a well clear violation and the severity, from a distance perspective, of a well clear violation. This metric is given by

$$d_{wc} = \begin{cases} \sqrt{h_{wc}^2 + v_{wc}^2} & h_{wc} > 0 \text{ and } v_{wc} > 0 \\ h_{wc} & h_{wc} > 0 \text{ and } v_{wc} < 0 \\ v_{wc} & v_{wc} > 0 \text{ and } h_{wc} < 0 \\ h_{wc} \text{ or } v_{wc} & h_{wc} < 0 \text{ and } v_{wc} < 0, \end{cases} \quad (1)$$

where h_{wc} and v_{wc} are the horizontal and vertical distances relative to the well clear volume

$$\begin{aligned} h_{wc} &= h - wc_h \\ v_{wc} &= v - wc_v, \end{aligned} \quad (2)$$

h and v are the horizontal and vertical distances between the two aircraft, and wc_h and wc_v are the sizes of the well clear volume in the horizontal and vertical directions. It is noted that if a well clear violation occurs (the last option in (1)], the value is determined according to the dimension that has the worst incursion towards the NMAC volume. The severity of the incursion towards NMAC was evaluated as the ratio of the distance from the well clear boundary divided by the distance from the well clear and NMAC boundaries (the incursion would be 1.0 for an aircraft at the NMAC boundary). Thus, if the most severe incursion towards the NMAC volume is in the horizontal direction, then d_{wc} is reported as v_{wc} , and vice-versa.

Another fundamental metric is Closest Point of Approach (CPA)

$$CPA = \min\left(\sqrt{h^2 + v^2}\right). \quad (3)$$

Depending upon the type of encounter, one may be interested in CPA in either the horizontal or vertical directions

$$\begin{aligned} CPA_h &= \min(|h|) \\ CPA_v &= \min(|v|). \end{aligned} \quad (4)$$

CPA_h is useful, for instance, for horizontal (type) encounters wherein a vertical aircraft offset is used to enhance safety.

The distance to well clear metrics (d_{wc} , h_{wc} , and v_{wc}) can be drawn from a time different from that of CPA. Herein, distance to well clear metrics were recorded from the time of the most severe violation. Thus, if a vertical well clear violation occurred early within the OEP, the distance-to-well-clear metrics would differ significantly from CPA metrics, especially for horizontal distances. It is useful to track both, as CPA can occur at a time that does not correspond with a violation—even a well clear violation. One example of this is an intruder tracing a relative path where it passes over, but just well clear of ownship, while descending such that it crosses the well clear boundary at a horizontal separation greater than its vertical separation when it passed over ownship. In that case, CPA occurs when the intruder is above ownship, but a well clear violation occurs later and further away from ownship.

3.1.1.4 Summary and DAA Steps

The A18 test plan “Small UAS Detect and Avoid Requirements Necessary for Limited Beyond Visual Line of Sight (BVLOS) Operations: Separation Requirements and Testing: (Overarching) Test Plan” suggests providing data in the following tables:

- Summary
- Detect (D) Step
- Track (T) Step
- Evaluate (E) Step
- Maneuver (M) Step

Because the risk ratio is used to summarize DAA system performance, some have suggested that provision of information regarding different DAA steps is not needed. However, it is expected that some level of detail regarding the DAA steps will be desired by those who evaluate test results. This has been reinforced by discussions held within the ASTM WK62669 DAA Test Methods Task Group.

Summary and DAA Steps data are illustrated using results from flight tests. Summary data are provided in two tables. Table 9 contains summary data for entire encounters, while Table 10 contains data from the OEPs. For all of the tables except OEP tables, the first seven columns provide text execution characteristics. The rest of the columns contain test results. Speed data (MA, UA, and closure speeds) are not provided in the OEP tables, and thus test result data begin in column 6 of those tables.

OEP tables are generated primarily to monitor aircraft altitude performance. The key metric is vertical aircraft separation. This is elucidated by providing information regarding aircraft

altitudes, separations, and altitude variability in Table 10. Aircraft altitude characteristics are further discussed in §4.3.

Example DTEM tables are provided in Tables 11-14. As illustrated in these tables, DAA event characteristics that are captured are:

- Detect: First detection
- Track: First target information reception, and track establishment
- Evaluate: Caution, warning, and maneuver identification
- Maneuver: Maneuver initiation and maneuver completion

DAA system characteristics that are captured are:

- Detect: Number of detections and False Target Rating (FTR)
- Track: Number of detections for track establishment
- Evaluate: Horizontal and vertical intruder location uncertainty at time of maneuver identification
- Maneuver: Maneuver type

Some values in Tables 11-14 are missing. This results either because log files for these variables were not evaluated in the interest of time (number of detections in Table 11 and horizontal and vertical intruder location uncertainty at time of maneuver identification in Table 13) or because the DAA system did not produce these variables (cautions and warnings in Table 13) owing to the use of ADS-B data and a vertical safety offset during tests. It is noted that the “H/V Unc Mvr ID” field could be filled in with non-missing values. However, since ADS-B data were used, the values can be estimated from GPS performance characteristics. Means for estimating this value is a continuing area of research.

First detection values as shown in Table 11 and first target information reception and track establishment values as shown in Table 12 were produced by leveraging the fact that for the encounters the intruder was always within the detection and tracking range of the system. These values represent the first point at which the intruder would be detected after the beginning of the encounter, the time when first detection data would be communicated to the tracker after the beginning of an encounter (with an assumed delay of 0 s), and the time when a track would be established after the beginning of an encounter. These assume a worst-case 1 s offset between ADS-B data reception and the timing of GPS puck data. In the DAA system utilized herein, 3 detections are required for track establishment (Brian Murray 2021, personal communication).

Table 9. Summary data for 23 September 2020 encounters. Abbreviated titles are: B. Time=encounter Begin Time; E. Time=encounter End Time; Intr./UAS Spd=INTRuder Speed/UAS Speed; H/V Cls. Spd=Closure Speed in the Horizontal and Vertical directions. Times are UTC (Universal Time Coordinated), speeds are in kts, Status indicates whether the encounter was acceptable (0=unacceptable, 1=acceptable), horizontal and vertical distances are in ft, and WCV (Well Clear Violation) indicates whether a well clear violation occurred and the type of violation (0=no violation, 1=well clear violation, 2=horizontal well clear violation, 3=vertical well clear violation). Speeds, including horizontal and vertical closure speeds (H/V Cls. Spd) are averages from the period when both aircraft are inbound to the HEFP. Large values consisting of the numeral ‘9’ indicate missing values.

Scen. ID	Date	B. Time	E. Time	Intr./UAS Spd	H/V Cls. Spd	Status	CPA _h	CPA _v	CPA	WCV	h _{wc}	v _{wc}	d _{wc}
HE-135-100	09/23/2020	1534:32	1536:03	85.02/ 36.45	67.86/ -1.14	1	6010.33	358.00	6020.98	0	4010.33	108.00	4011.78
HE-270-100	09/23/2020	1540:13	1542:09	104.80/ 37.07	109.77/ -0.09	1	3482.16	292.00	3494.39	0	1482.16	42.00	1482.76
HE-45-100	09/23/2020	1544:37	1546:53	84.44/ 45.57	121.20/ -1.89	1	5278.90	282.00	5286.43	3	17101.65	-58.00	17101.65
HE-180-100	09/23/2020	1550:14	1552:10	106.74/ 54.52	50.99/ 0.03	1	825.52	375.00	906.70	2	-1174.48	125.00	125.00
HE-90-100	09/23/2020	1554:56	1555:58	82.39/ 33.42	79.42/ -1.00	1	7670.83	366.00	7679.56	0	5670.83	116.00	5672.02
HE-225-100	09/23/2020	1558:57	1600:34	106.97/ 43.65	86.45/ -1.71	1	2226.45	336.00	2251.66	0	226.45	86.00	242.23
HE-45-100	09/23/2020	1602:28	1604:42	79.97/ 48.41	113.84/ 0.65	1	4448.77	303.00	4459.08	0	2448.77	53.00	2449.34

Table 10. OEP Summary data for 23 September 2020 encounters. Abbreviated titles are OEP BTime=OEP Beginning Time; OEP ETime=OEP End Time; Min h_{dist}=Minimum Horizontal DISTance between aircraft; UA Mean/Max-Mean/Mean-Min=UA MEAN height (AGL)/MAXimum height – MEAN height/MEAN height – MINimum height; MA Mean/Max-Mean/Mean-Min=MA MEAN height (AGL)/MAXimum height – MEAN height/MEAN height – MINimum height; Diff. Mean/Max/Min=MEAN/MAXimum/MINimum of aircraft height DIFFerences. Times, Status, and distance units are as in Table 9. Large values consisting of the numeral ‘9’ indicate missing values.

Scen. ID	Date	OEP BTime	OEP ETime	Status	Min h _{dist}	UA Mean/Max-Mean/Mean-Min	MA Mean/Max-Mean/Mean-Min	Diff. Mean/Max/Min
HE-135-100	09/23/2020	1535:03	1535:49	1	6010.33	313.89/12.11/7.89	650.21/17.79/19.21	336.32/362.00/305.00
HE-270-100	09/23/2020	1540:31	1541:49	1	3482.16	317.32/10.68/8.32	616.70/37.30/41.70	299.38/331.00/265.00
HE-45-100	09/23/2020	1544:54	1546:43	1	5278.90	322.16/13.84/11.16	601.46/26.54/90.46	279.30/309.00/192.00
HE-180-100	09/23/2020	1550:34	1551:51	1	825.52	315.26/18.74/16.26	648.23/68.77/48.23	332.97/417.00/279.00
HE-90-100	09/23/2020	1554:57	1555:44	1	7670.83	315.25/13.75/11.25	637.31/50.69/49.31	322.06/378.00/268.00
HE-225-100	09/23/2020	1559:22	1600:16	1	2226.45	318.05/6.95/6.05	652.78/27.22/28.78	334.73/367.00/306.00
HE-45-100	09/23/2020	1603:21	1604:27	1	4448.77	337.18/19.82/30.18	622.73/27.27/19.73	285.55/324.00/254.00

Table 11. Detect (D) step data for 23 September 2020 encounters. Abbreviated titles are as in Table 9, with the additional abbreviations H/V Dist 1st Det=Horizontal/Vertical DISTances between aircraft at the time of 1st DETection; T1Det=Time of 1st DETection; # Det=Number of DETections during the encounter; FTR=False Target Rating [0=false targets not present, 1=false targets present but no factor, 2=false targets present and impacted system (e.g., delayed track establishment or track accuracy), 3=false targets prevented identification of actual target]. Times, Status, and distance units are as in Table 9. Large values consisting of the numeral ‘9’ indicate missing values.

Scen. ID	Date	B. Time	E. Time	Intr./UAS Spd	H/V Cls. Spd	Status	H/V Dist 1 st Det	T1Det	# Det	FTR
HE-135-100	09/23/2020	1534:32	1536:03	85.02/ 36.45	67.86/ -1.14	1	13232.32/ 275.00	1534:33	999999	1
HE-270-100	09/23/2020	1540:13	1542:09	104.80/ 37.07	109.77/ -0.09	1	14986.16/ 288.00	1540:14	999999	1
HE-45-100	09/23/2020	1544:37	1546:53	84.44/ 45.57	121.20/ -1.89	1	21533.94/ 318.00	1544:38	999999	1
HE-180-100	09/23/2020	1550:14	1552:10	106.74/ 54.52	50.99/ 0.03	1	5880.73/ 318.00	1550:15	999999	1
HE-90-100	09/23/2020	1554:56	1555:58	82.39/ 33.42	79.42/ -1.00	1	11612.06/ 273.00	1554:57	999999	1
HE-225-100	09/23/2020	1558:57	1600:34	106.97/ 43.65	86.45/ -1.71	1	11365.50/ 343.00	1558:58	999999	1
HE-45-100	09/23/2020	1602:28	1604:42	79.97/ 48.41	113.84/ 0.65	1	20205.77/ 328.00	1602:29	999999	1

Table 12. Track (T) step data for 23 September 2020 encounters. Abbreviated titles are as in Table 9, with the additional abbreviations Time/H/V Dist 1st TInfo=Time and Horizontal and Vertical DISTances between aircraft when 1st Target Information is received by the tracker; Time/H/V Dist Trk Establ=Time and Horizontal and Vertical DISTances between aircraft when a TRacK was ESTABLISHED; # Det=Number of DETections for track establishment. Times, Status, and distance units are as in Table 9. Large values consisting of the numeral ‘9’ indicate missing values.

Scen. ID	Date	B. Time	E. Time	Intr./UAS Spd	H/V Cls. Spd	Status	Time/H/V Dist 1 st TInfo	Time/H/V Dist Trk Establ	# Det
HE-135-100	09/23/2020	1534:32	1536:03	85.02/ 36.45	67.86/ -1.14	1	1534:33/ 13232.32/ 275.00	1534:36/ 12781.68/ 253.00	3
HE-270-100	09/23/2020	1540:13	1542:09	104.80/ 37.07	109.77/ -0.09	1	1540:14/ 14986.16/ 288.00	1540:17/ 15325.77/ 287.00	3
HE-45-100	09/23/2020	1544:37	1546:53	84.44/ 45.57	121.20/ -1.89	1	1544:38/ 21533.94/ 318.00	1544:41/ 21529.34/ 311.00	3
HE-180-100	09/23/2020	1550:14	1552:10	106.74/ 54.52	50.99/ 0.03	1	1550:15/ 5880.73/ 318.00	1550:18/ 6523.06/ 349.00	3
HE-90-100	09/23/2020	1554:56	1555:58	82.39/ 33.42	79.42/ -1.00	1	1554:57/ 11612.06/ 273.00	1555:00/ 11233.55/ 282.00	3
HE-225-100	09/23/2020	1558:57	1600:34	106.97/ 43.65	86.45/ -1.71	1	1558:58/ 11365.50/ 343.00	1559:01/ 11368.68/ 293.00	3
HE-45-100	09/23/2020	1602:28	1604:42	79.97/ 48.41	113.84/ 0.65	1	1602:29/ 20205.77/ 328.00	1602:32/ 20564.67/ 300.00	3

Table 13. Evaluate (E) step data for 23 September 2020 encounters. Abbreviated titles are as in Table 9, with the additional abbreviations Dt from EB/H/V Caution=Time difference (seconds) from Encounter Begin and Horizontal and Vertical aircraft separation at the time of CAUTION issuance; Dt from EB/H/V Warning=Time difference (seconds) from Encounter Begin and Horizontal and Vertical aircraft separation at the time of WARNING issuance; Dt from EB/H/V Mvr ID=Time difference (seconds) from Encounter Begin and Horizontal and Vertical aircraft separation at the time of ManeuVeR IDentification; H/V Unc Mvr ID=Uncertainty in intruder Horizontal and Vertical locations at the time of ManeuVeR IDentification. Times, Status, and distance units are as in Table 9. Large values consisting of the numeral ‘9’ indicate missing values.

Scen. ID	Date	B. Time	E. Time	Intr./UAS Spd	H/V Cls. Spd	Status	Dt from EB/H/V Caution	Dt from EB/H/V Warning	Dt from EB/H/V Mvr ID	H/V Unc Mvr ID
HE-135-100	09/23/2020	1534:32	1536:03	85.02/ 36.45	67.86/ -1.14	1	999999/ 99999999/ 99999999	999999/ 99999999/ 99999999	39.00/ 8054.66/ 325.00	9999999/ 9999999
HE-270-100	09/23/2020	1540:13	1542:09	104.80/ 37.07	109.77/ -0.09	1	999999/ 99999999/ 99999999	999999/ 99999999/ 99999999	60.00/ 7157.50/ 329.00	9999999/ 9999999
HE-45-100	09/23/2020	1544:37	1546:53	84.44/ 45.57	121.20/ -1.89	1	999999/ 99999999/ 99999999	999999/ 99999999/ 99999999	55.00/ 11932.44/ 281.00	9999999/ 9999999
HE-180-100	09/23/2020	1550:14	1552:10	106.74/ 54.52	50.99/ 0.03	1	999999/ 99999999/ 99999999	999999/ 99999999/ 99999999	50.00/ 4387.07/ 306.00	9999999/ 9999999
HE-90-100	09/23/2020	1554:56	1555:58	82.39/ 33.42	79.42/ -1.00	1	999999/ 99999999/ 99999999	999999/ 99999999/ 99999999	16.00/ 9623.23/ 278.00	9999999/ 9999999
HE-225-100	09/23/2020	1558:57	1600:34	106.97/ 43.65	86.45/ -1.71	1	999999/ 99999999/ 99999999	999999/ 99999999/ 99999999	45.00/ 4924.10/ 318.00	9999999/ 9999999
HE-45-100	09/23/2020	1602:28	1604:42	79.97/ 48.41	113.84/ 0.65	1	999999/ 99999999/ 99999999	999999/ 99999999/ 99999999	64.00/ 12537.17/ 319.00	9999999/ 9999999

Table 14. Maneuver (M) step data for 23 September 2020 encounters. Abbreviated titles are as in Table 9, with the additional abbreviations Time/H/V Dist Mvr Init=Time and Horizontal and Vertical aircraft separation/DISTances at the time of ManeuVeR INITiation; Time/H/V Dist Mvr Comp=Time and Horizontal and Vertical aircraft separation/DISTances at the time of ManeuVeR COMpletion; Mvr Type=ManeuVeR TYPE ('L'=left turn, 'R'=right turn, 'C'=climb, 'D'=descend). Times, Status, and distance units are as in Table 9. Large values consisting of the numeral '9' indicate missing values.

Scen. ID	Date	B. Time	E. Time	Intr./UAS Spd	H/V Cls. Spd	Status	Time/H/V Dist Mvr Init	Time/H/V Dist Mvr Comp	Mvr Type
HE-135-100	09/23/2020	1534:32	1536:03	85.02/ 36.45	67.86/ -1.14	1	1535:18/ 7278.73/ 323.00	1535:50/ 6014.72/ 354.00	L
HE-270-100	09/23/2020	1540:13	1542:09	104.80/ 37.07	109.77/ -0.09	1	1541:15/ 6775.48/ 326.00	1541:42/ 3491.61/ 296.00	L
HE-45-100	09/23/2020	1544:37	1546:53	84.44/ 45.57	121.20/ -1.89	1	1545:40/ 10343.68/ 300.00	1546:44/ 5283.12/ 283.00	L
HE-180-100	09/23/2020	1550:14	1552:10	106.74/ 54.52	50.99/ 0.03	1	1551:13/ 3646.88/ 319.00	1551:42/ 2109.50/ 402.00	R
HE-90-100	09/23/2020	1554:56	1555:58	82.39/ 33.42	79.42/ -1.00	1	1555:18/ 8791.49/ 301.00	1555:45/ 7671.48/ 364.00	L
HE-225-100	09/23/2020	1558:57	1600:34	106.97/ 43.65	86.45/ -1.71	1	1559:47/ 4212.25/ 352.00	1600:03/ 2231.89/ 339.00	L
HE-45-100	09/23/2020	1602:28	1604:42	79.97/ 48.41	113.84/ 0.65	1	1603:39/ 11154.10/ 306.00	1604:28/ 4451.49/ 304.00	R

3.1.1.5 Separation Timeline

The fundamental metrics associated with DAA commonly reduce to separation and timing. A means for illustrating these was developed and labelled as a separation timeline, which is a plot of aircraft separation as a function of time. The time variable utilized herein is seconds prior to unmitigated CPA, which would occur if neither aircraft maneuvered and continued to fly the heading and speed utilized during their inbound segment. Because aircraft headings and speeds varied during the inbound segments, the smallest (“best case”) unmitigated CPA was utilized. For horizontal encounters as executed herein, unmitigated CPA_h and horizontal separations are utilized. For encounters that include closure in the vertical direction, CPA and total separation are utilized.

3.1.1.5.1 2D (Horizontal) Unmitigated CPA (CPA_h) Derivation

The challenge is to develop relations for determining when two aircraft that are flying along straight paths will reach their horizontal Closest Point of Approach (CPA_h). For simplicity, distances are treated as arc-distances along a spherical Earth with no correction to the radius of the associated arc-distances for east-west travel as the aircraft move north-south. Distances from a reference longitude and latitude (λ_r, ϕ_r) are given by

$$x = R \cos \phi_r (\lambda_r - \lambda) \quad (5)$$

and

$$y = R(\phi - \phi_r), \quad (6)$$

where x is the approximate east-west distance, y is the approximate north-south distance, R is the radius of the earth, longitude λ is assumed to be measured relative to “west” (e.g., 97° W), and latitude ϕ is measured relative to “north” (e.g., 45° N). It is noted that (5) and (6) approximate distances in the east-west and north-south directions from the arc-length distance relation $\Delta s = r\Delta\theta$, where s is arc-length, r is radius, and θ is the angular distance in radians. Thus, the longitude and latitude differences in (5) and (6) must be in radians.

Given that the two aircraft considered herein are not maneuvering and are assumed to be maintaining constant speed, their speeds in both the x and y directions are constant. Thus, the position of these two aircraft—the Unmanned Aircraft (UA) and Manned Aircraft (MA), are given by

$$x_{UA} = x_{UA0} + u_{UA}t \quad (7)$$

$$y_{UA} = y_{UA0} + v_{UA}t \quad (8)$$

$$x_{MA} = x_{MA0} + u_{MA}t \quad (9)$$

$$y_{MA} = y_{MA0} + v_{MA}t, \quad (10)$$

where subscript 0 indicates location at time $t=0$ and u and v are speeds in the x and y directions. Thus, these assume that the arc-distances in the east-west and north-south directions of the aircraft (relative to a reference point) change linearly with time. *It is noted that this is an approximation for the east-west direction, since the $\cos\phi$ term in (1) should evolve with time as the latitude of the aircraft changes.*

The horizontal distance between the two aircraft is a function of time and is given by

$$d_h(t) = \sqrt{(x_{MA} - x_{UA})^2 + (y_{MA} - y_{UA})^2} \quad (11)$$

$$= \sqrt{[(x_{MA0} - x_{UA0}) + (u_{MA} - u_{UA})t]^2 + [(y_{MA0} - y_{UA0}) + (v_{MA} - v_{UA})t]^2}.$$

For convenience, the quantity $d_h^2(t)$ will be utilized

$$d_h^2(t) = [(x_{MA0} - x_{UA0}) + (u_{MA} - u_{UA})t]^2 + [(y_{MA0} - y_{UA0}) + (v_{MA} - v_{UA})t]^2. \quad (12)$$

CPA_h occurs when d_h is a minimum. At this point, since $d_h \geq 0$, d_h^2 is also a minimum. Thus, the time of CPA_h is determined by taking the derivative of (12) with respect to time and setting the result to zero:

$$\frac{d[d_h^2(t)]}{dt} = \quad (13)$$

$$2(u_{MA} - u_{UA})[(x_{MA0} - x_{UA0}) + (u_{MA} - u_{UA})t] + 2(v_{MA} - v_{UA})[(y_{MA0} - y_{UA0}) + (v_{MA} - v_{UA})t] = 0$$

Solving for t results in

$$[(u_{MA} - u_{UA})^2 + (v_{MA} - v_{UA})^2]t = -(u_{MA} - u_{UA})(x_{MA0} - x_{UA0}) - (v_{MA} - v_{UA})(y_{MA0} - y_{UA0}) \quad (14)$$

$$t = \frac{-(u_{MA} - u_{UA})(x_{MA0} - x_{UA0}) - (v_{MA} - v_{UA})(y_{MA0} - y_{UA0})}{(u_{MA} - u_{UA})^2 + (v_{MA} - v_{UA})^2}. \quad (15)$$

3.1.1.5.2 3D Unmitigated CPA Derivation

Extending the previous derivation to three dimensions, aircraft positions are given by

$$x_{UA} = x_{UA0} + u_{UA}t \quad (16)$$

$$y_{UA} = y_{UA0} + v_{UA}t \quad (17)$$

$$h_{UA} = h_{UA0} + w_{UA}t \quad (18)$$

$$x_{MA} = x_{MA0} + u_{MA}t \quad (19)$$

$$y_{MA} = y_{MA0} + v_{MA}t \quad (20)$$

$$h_{MA} = h_{MA0} + w_{MA}t, \quad (21)$$

where it is assumed that both aircraft are flown with constant east-west (u) and north-south (v) speeds and with constant vertical speeds w . With these, the distance between the two aircraft is the function of time

$$d(t) = \sqrt{(x_{MA} - x_{UA})^2 + (y_{MA} - y_{UA})^2 + (h_{MA} - h_{UA})^2} \quad (22)$$

$$= \sqrt{[(x_{MA0} - x_{UA0}) + (u_{MA} - u_{UA})t]^2 + [(y_{MA0} - y_{UA0}) + (v_{MA} - v_{UA})t]^2 + [(h_{MA0} - h_{UA0}) + (w_{MA} - w_{UA})t]^2}.$$

For convenience, the quantity $d^2(t)$ is utilized

$$d^2(t) = \left[(x_{MA0} - x_{UA0}) + (u_{MA} - u_{UA})t \right]^2 + \left[(y_{MA0} - y_{UA0}) + (v_{MA} - v_{UA})t \right]^2 + \left[(h_{MA0} - h_{UA0}) + (w_{MA} - w_{UA})t \right]^2. \quad (23)$$

CPA occurs when d is a minimum. At this point, since $d \geq 0$, d^2 is also a minimum. Thus, the time of CPA is determined by taking the derivative of (23) with respect to time and setting the result to zero:

$$\frac{d[d^2(t)]}{dt} = 2(u_{MA} - u_{UA})[(x_{MA0} - x_{UA0}) + (u_{MA} - u_{UA})t] + 2(v_{MA} - v_{UA})[(y_{MA0} - y_{UA0}) + (v_{MA} - v_{UA})t] + 2(w_{MA} - w_{UA})[(h_{MA0} - h_{UA0}) + (w_{MA} - w_{UA})t] = 0. \quad (24)$$

Solving for t produces

$$\left[(u_{MA} - u_{UA})^2 + (v_{MA} - v_{UA})^2 + (w_{MA} - w_{UA})^2 \right] t = -(u_{MA} - u_{UA})(x_{MA0} - x_{UA0}) - (v_{MA} - v_{UA})(y_{MA0} - y_{UA0}) - (w_{MA} - w_{UA})(h_{MA0} - h_{UA0}). \quad (25)$$

$$t = \frac{-(u_{MA} - u_{UA})(x_{MA0} - x_{UA0}) - (v_{MA} - v_{UA})(y_{MA0} - y_{UA0}) - (w_{MA} - w_{UA})(h_{MA0} - h_{UA0})}{(u_{MA} - u_{UA})^2 + (v_{MA} - v_{UA})^2 + (w_{MA} - w_{UA})^2}. \quad (26)$$

3.1.1.5.3 Evaluation of Unmitigated CPA_h Accuracy

For horizontal encounters, (15) has been used to estimate the time of CPA_h and (11) [leveraging (7)-(10)] has been used to estimate CPA_h. To estimate the error associated with use of (15) and (11), the distances between the two aircraft estimated using great circle distance equations (i.e., assuming a spherical Earth) for the time of travel given by (15) and the heading and speeds provided by the GPS pucks, GCC_h, were computed. A comparison between the two is provided in Table 15.

Table 15. Examples of CPA_h errors from the September 2020 flight tests. Times to CPA_h are estimated using the method derived herein and aircraft separation is evaluated using the method derived herein (11) and great circle distance equations (GCC_h).

UA Heading ($^{\circ}$)	UA Speed (ft s^{-1})	MA Heading ($^{\circ}$)	MA Speed (ft s^{-1})	CPA_h from (11) (ft)	GCC_h (ft)	$GCC_h - CPA_h$ (ft)	% Error
10.83	94.97	338.04	171.9	3131.36	3136.10	3.74	0.12
63.58	89.04	146.5	140.11	1936.85	1937.17	0.32	0.016
99.35	63.8	333.5	173.91	2469.09	2468.68	-0.41	-0.0117
98.22	62.69	323.09	170.38	187.42	188.42	0.995	0.53
146.48	48.17	135.00	152.53	814.23	813.66	-0.57	-0.07
10.28	86.09	342.00	182.62	80.96	79.85	-1.1	-1.39
10.04	85.40	341.10	183.18	60.11	61.22	1.11	1.81
100.96	79.28	147.72	158.73	1.77	1.97	0.20	10.3
327.48	88.31	149.59	142.88	953.21	953.30	0.087	0.00907

For the September 2020 tests the minimum and maximum errors ($GCC_h - CPA_h$) are -2.1 ft and 3.74 ft. Thus, these differences appear to be bounded by ~ 5 ft. For this week of tests, the lowest horizontal closure speeds for the two aircraft were 38.93 kts (65.71 ft s^{-1}) for the 80 kt encounters (intruder speed) and 50.99 kts (86.06 ft s^{-1}) for the 100 kt encounters (intruder speed). These correspond to temporal errors of 0.076 s and 0.058 s. Thus, the times computed using (15) are estimated to be accurate to within ~ 0.1 s. The spatial error associated with CPA_h (~ 5 ft) is easily within the required 95% GPS WAAS horizontal performance (16 m) and is about twice the observed 95% GPS WAAS horizontal performance (0.63 m) (FAA 2021). For reference, standard GPS 95% performance numbers are 36 m (required) and 2.9 m (observed).⁶

3.1.2 Campaign Metrics

3.1.2.1 (Sample) Risk Ratio

The loss of well clear risk ratio LR is given by

$$LR = \frac{\sum_{i=1}^N I_i n_i LR_i}{\sum_{i=1}^N I_i n_i}, \quad (27)$$

where LR_i is the loss of well clear risk ratio for the i^{th} encounter geometry, n_i is the number of encounters for the i^{th} geometry, and I_i is a weighting factor that allows one to apply more weight to certain encounter geometries than others. The latter might be utilized, for instance, if certain geometries are determined to be more likely (or important) than other geometries. Herein, $I_i=1$. It is noted that one could give certain geometries more weight than others by executing more encounters (greater n_i) for those geometries.

⁶ A previous version of the web page FAA (2021) provided these numerical values.

Because the encounters that were executed for these tests utilized ‘collision’ geometries and were horizontal encounters, the variable estimated herein is

$$LR_{ch} = \frac{\sum_{i=1}^N I_i n_i LR_{ch_i}}{\sum_{i=1}^N I_i n_i}, \quad (28)$$

where LR_{ch_i} is the loss of well clear sample risk ratio for the i^{th} ‘collision’ horizontal geometry.

3.1.2.2 Sample Risk Ratio Uncertainty

Understanding uncertainties associated with LR_{ch} is important, as they provide context regarding the potential range of values and whether values are consistent with other estimation methods (e.g., simulation). Multiple approaches to estimating uncertainty have been investigated. These are divided according to whether it is assumed that encounter characteristics depend upon encounter geometry (non-homogenous) or whether they are independent of encounter geometry (homogeneous).

3.1.2.2.1 Non-Homogeneous

The first approach to estimating uncertainties is based upon the assumption that encounter characteristics depend upon encounter geometry. It was developed using CPA_h values. For each encounter geometry, the distribution of CPA_h values was fit using a Truncated Normal distribution (Burkardt 2014). A parametric approach (assumed distribution) is used, as initial research did not reveal an appropriate non-parametric approach. A Normal distribution was assumed for the basic underlying shape based upon tests conducted with the data. The first test utilized is the D’Agostino (1971) and D’Agostino and Pearson (1973) test that combines skew and kurtosis to test normality. This test provides a probability p (a χ^2 probability) that the sample comes from a Normal distribution. If this value is very low, the hypothesis that a sample comes from a Normal distribution can be rejected. In order to have enough values to justify such a test, all CPA_h values for each speed tested (80 kts and 100 kts), which encompass horizontal encounter geometries ranging from 0° - 360° degrees sampled every 45° for each speed, were used in the test.⁷ The results for the two sets of tests are:

- 80 kts: $p = 0.58$
- 100 kts: $p = 0.37$

Thus, the null hypothesis that the values come from a Normal distribution is not rejected. The second test involved identifying the best distribution that fits the data. The possible distributions that are evaluated are:

- Normal
- Exponential Weibull
- Weibull Minimum Extreme Value
- Weibull Maximum Extreme Value
- Pareto

⁷ It is noted that for the purpose of this test this is treating the values as homogeneous with respect to encounter geometry.

- Generalized Extreme (combines Gumbel, Fréchet, and Weibull families)

These are distributions available in the Python 3 SciPy library (Virtanen et al. 2020). The results for the two speeds are:

- 80 kts: Generalized Extreme
- 100 kts: Normal

While the best fit for 80 kts was the Generalized Extreme distribution, the normality test for 80 kts was far from rejecting the null hypothesis that the same comes from a Normal distribution. Thus, assumption of a fundamentally-normal shape is justified.

A Truncated Normal Distribution is utilized because CPA_h values are truncated at 0 ft and at the maximum separation distance experienced during the encounters, which was estimated as 20,833 ft (the maximum initial separation for the encounter set). The impact of truncation is transferal of probability from beyond the truncation point in the Normal distribution to the region within the truncation limits, as illustrated in Figure 14. As shown in this figure, truncation results in zero probability beyond truncation points and in a higher peak in the distribution. It is noted that this example is derived from test data (CPA_h values for 100 kts encounter speed and 180° encounter geometry). Examination of those data indicate that the upper truncation has little effect for those data, while the lower truncation has an important effect (as indicated in Figure 14). Because the lower truncation shifts probability density such that the loss of probability density for $CPA_h < 2000$ ft from the normal distribution is greater than the gain in the 0-2000 ft range in the Truncated Normal distribution, truncation decreases LR_{ch} . For the example shown, which is from the geometry expected to experience the greatest truncation impact for the 100 kt tests because the CPA_h values are collectively the smallest (closest to the 0 ft truncation), the cumulative probability that $CPA_h \leq 2000$ ft is 0.636 for the Normal distribution and 0.604 for the Truncated Normal Distribution. Thus, the effect of truncation on the cumulative probability of a horizontal well clear violation is neither dominating nor negligible.

For the Truncated Normal distributions, which were generated for each encounter geometry for each speed if at least three or more CPA_h values were available for all encounter geometries at a given speed, mean and standard deviations were computed using the traditional formulations

$$\mu_q = \frac{\sum_{i=1}^N q_i}{N}, \quad (29)$$

and

$$\sigma_q = \sqrt{\frac{\sum_{i=1}^N (q_i - \mu_q)^2}{N-1}}, \quad (30)$$

where q is a general quantity, μ indicates an average value, σ indicates a standard deviation value, and N is the total number of samples. The more complicated estimators for these quantities that apply for a Truncated Normal distribution (Burkardt 2014) are not used because, with the exception of extreme cases of truncation, the more simple estimators (29)-(30) provide accurate results for the Truncated Normal distribution (Barr and Sherrill 1999).

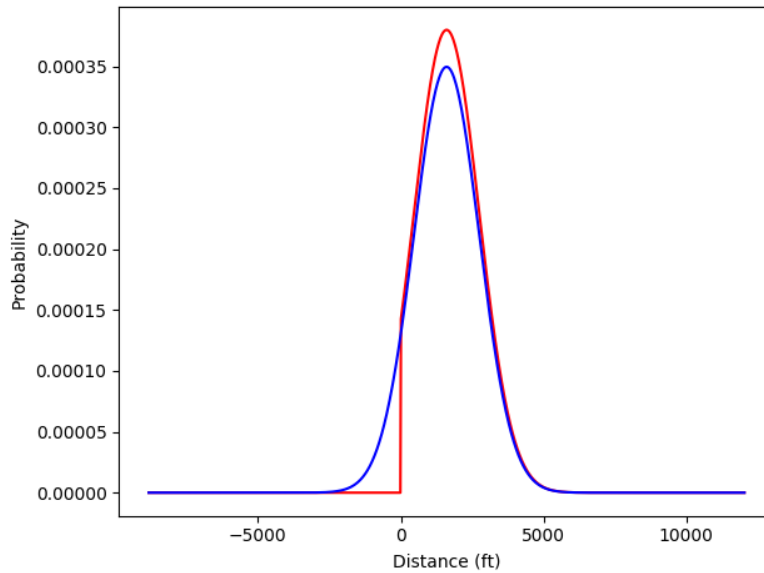


Figure 14. Illustration of the difference between a Normal (blue line) and Truncated Normal distribution (red line). Distribution parameters are $\mu = 1604.24$ ft and $\sigma=1140.85$ ft, with truncation in the Truncated Normal Distribution at 0 ft and 20,833 ft. These parameters are derived from CPA_h values for 100 kts encounter speed and 180° encounter geometry, which were generated using the collision geometries with vertical safety offset and DAA approach described herein as opposed to unmitigated encounters or simulated results like those used to estimate risk ratios.

For each encounter geometry (at each speed), three Truncated Normal distributions are generated: one directly from the data, a best-case distribution, and a worst-case distribution. The best-case and worst-case distributions are Truncated Normal distributions that have means and standard deviations $(\mu + \sigma_\mu, \sigma - \sigma_\sigma)$ and $(\mu - \sigma_\mu, \sigma + \sigma_\sigma)$, respectively. The variables σ_μ and σ_σ are the standard deviations of the mean and of the standard deviation, and are given by (Taylor 1996)

$$\sigma_\mu = \frac{\sigma}{\sqrt{N}} \quad (31)$$

and

$$\sigma_\sigma = \frac{\sigma}{\sqrt{2(N-1)}}. \quad (32)$$

An example corresponding to Figure 14 is shown in Figure 15.

Once the three Truncated Normal distributions are formed for an encounter geometry, the cumulative probability of $CPA_h \leq 2000$ ft is computed for each of them. This is repeated for each encounter geometry, and then three LR_{ch} values are computed using these Truncated Normal distributions using (28), one for the cumulative probabilities for the distributions derived directly

from the data, one for the cumulative probabilities for the best-case distributions, and one for the cumulative probabilities for the worst-case distributions. This produces three LR_{ch} values. From this, the difference in LR_{ch} between the worst-case and best-case results and the value estimated from the distributions derived directly from the data are computed and are used as the “deltas” for the uncertainty range. These deltas are then added/subtracted to/from LR_{ch} computed directly from the data (without utilizing a distribution) using (28). It is noted that deltas are used because the LR_{ch} value computed with the cumulative probabilities from Truncated Normal distributions derived directly from the data in (28) is not perfectly equal to the LR_{ch} value computed directly from the data using (28). For the 100 kt tests conducted in September 2020, $LR_{ch} = 0.26$ when computed directly from the data (without using a distribution) and $LR_{ch} = 0.21$ when computed using the cumulative probabilities from Truncated Normal distributions (derived directly from the data).

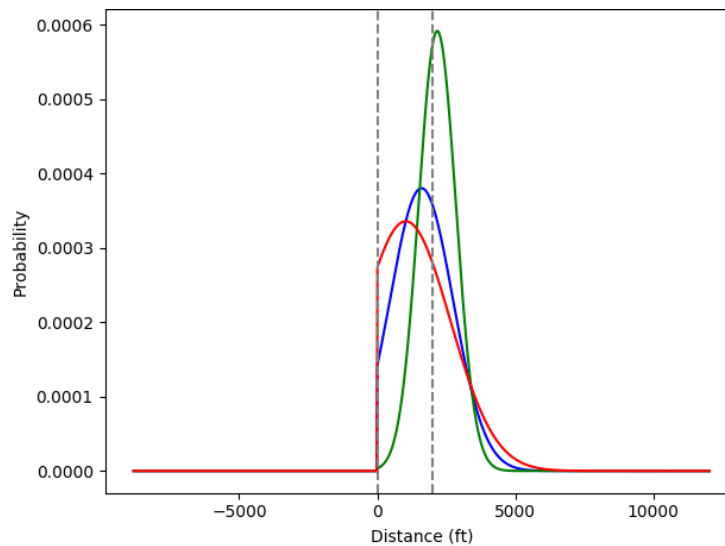


Figure 15. Illustration of best-case (green) and worst-case (red) Truncated Normal distributions. Distributions were generated from the data upon which Figure 14 was produced. The blue line is the Truncated Normal distribution based upon the data and corresponds to the red line in Figure 14.

3.1.2.2.2 Homogeneous

Two approaches were explored for the situation where statistical properties for CPA_h do not depend upon encounter geometry. The first was suggested by Ben Thein of Scientific Applications and Research Associates, Inc. (Ben Thein 2021, personal communication). This utilizes a binomial proportion confidence interval, which is a confidence interval for the probability of an outcome calculated from a series of success-failure (binary) experiments. Herein, the approach developed by Wilson (1927) was utilized. This method applies the fundamental assumption that the error in the number of outcomes (success or failures) is normally distributed, which can break down when the number of samples is small. Unlike a related method, however, the Wilson (1927) approach has good properties even for a small number of samples and for extreme probabilities (i.e., close

to 0 or 1) (Wikipedia 2021). It is noted that the continuity correction (Newcombe 1998) was not applied.

The second approach was suggested by Adam Hendrickson from the FAA (Adam Hendrickson 2021, personal communication). In this method, a Normal distribution is formed from all CPA_h values for all encounter geometries for a test speed. Then, best- and worst-case distributions are formed as with the non-homogeneous method, but for all CPA_h values for all encounter geometries for a test speed. Cumulative Density Functions (CDFs) for the three distributions are then used to estimate LR_{ch} and the upper (worst-case) and lower (best-case) values associated with the confidence interval. A variation to this approach involves use of a Truncated Normal distribution. This has not been attempted yet, but will be in the near future.

3.2 Software

3.2.1 Language

Because of the need to produce results quickly and because of its rich, publicly-available software set, Python 3 (Van Rossum and Drake 2009) was used. It is noted that numerous software modules, including visualization and a module for performing great circle calculations, were utilized.

3.2.2 Organization

Two sets of software were developed—software for processing individual encounters and software for producing overall campaign results. For convenience, the encounter processing occurs for each flight test day. Thus, the software sets are referred to as ‘ByDay’ and ‘Campaign’.

3.2.2.1 ByDay Software

The processing flow is:

- Obtain/set program control variables
- Check program invocation
- Obtain DCAPS data
 - Delineates encounters
 - Provides additional information such as when the EO identified the maneuver
- Obtain aircraft position data (GPS puck data)
- Obtain ADS-B data for the manned aircraft (if requested)
- Compute encounter events, statistics, and characteristics
 - Determine when aircraft are inbound
 - Identify encounter events and compute distance metrics
 - Loss/regain of well clear, horizontal well clear, and vertical well clear
 - Aircraft horizontal and vertical separation as a function of time
 - CPA, CPA_h , and CPA_v
 - Identify the OEP
 - Compute additional distance metrics and refine encounter events
 - d_{wc} , h_{wc} , and v_{wc}
 - Refine vertical well clear data using OEP
 - Determine times of loss/regain of well clear, horizontal well clear, and vertical well clear
 - Compute metrics that are relevant when both aircraft are inbound
 - Determine when both aircraft are inbound

- Compute average speeds for each aircraft when both are inbound
 - Compute closure speeds (horizontal and vertical) while both aircraft are inbound
 - Compute height statistics
 - Aircraft maximum and minimum heights during encounters
 - Aircraft maximum, minimum, and mean heights during the OEP
 - Compute minimum horizontal aircraft separation during the OEP
- Compute DTEM statistics
 - Compute Detect statistics
 - Compute Track statistics
 - Compute Evaluate statistics
 - Compute Maneuver statistics
- Compute separation timeline statistics
 - Compute unmitigated CPA or CPA_h
 - Compute aircraft distances and times prior to unmitigated CPA from when both aircraft are inbound to the end of the OEP
 - Compute aircraft distances and times prior to unmitigated CPA for encounter descriptors (e.g., when both aircraft are inbound) and DTEM DAA event characteristics (first detection, maneuver initiation, etc.).
- Output summary results to files
 - Output to text files
 - Output to Microsoft® Word® compatible files
- Output DTEM results to files
 - Output to text files
 - Output to Microsoft® Word® compatible files
- Create “XY” plots (described in results section)
- Create box plots (described in results section)
- Create overview plots (described in results section)
- Create separation timeline plots

3.2.2.2 Campaign Software

The processing flow is:

- Set program control variables
- Check program invocation
- Ingest encounter summary (overview and OEP) data (produced using ByDay software)
- Organize the summary data according to encounter type, test speed, and encounter geometry/angle
- Compute statistics
 - Compute maximum, minimum, mean, median, and standard deviation of CPA_h value groups (grouped by encounter type, test speed, and encounter geometry/angle)
 - Compute LR_{ch} for CPA_h value groups
 - Test distribution of CPA_h values grouped by encounter type and test speed for normality

- Determine which distribution best fits CPA_h values grouped by encounter type and test speed
- Estimate LR_{ch} uncertainty using the non-homogeneous method
- Estimate LR_{ch} uncertainty using the homogeneous binomial proportion confidence interval
- Create plots
 - Plot encounter events
 - Create distance vs. encounter angle plots (described in results section)
 - Create density function plots
 - Cumulative Density Function (CDF; from data)
 - Theoretical CDF (from statistical properties of data)
 - Best and worst-case CDFs and associated values at the well-clear boundary (second homogeneous uncertainty estimation method)
 - Theoretical Probability Density Function (PDF; from statistical properties of data)

4 TEST RESULTS

4.1 Flight Summary

A summary of the encounter set is provided in Table 16. As indicated, 63 encounters were desired. This resulted from 5 encounters for 100 kt intruder speed at 8 angles plus 5 extra encounters utilized to leverage the rotation of the origin direction of the MA (NW and SE) forming 45 encounters for 100 kts and 2 encounters for 80 kt intruder speed at 8 angles plus 2 extra encounters utilized to leverage the rotation of the origin direction of the MA (NW and SE) forming 18 encounters for 80 kts.

Table 16. Summary of September 2020 flight test encounters.

Day	Number of Encounters	Comments
Monday	0	Shakedown in morning. Wind limits in afternoon.
Tuesday	20	2 not acceptable. 1 rerun Tuesday, other Friday.
Wednesday	7	Wind limits in afternoon.
Thursday	14	Fog until late in the day. 1 not acceptable.
Friday	28	1 not acceptable. Fit between rain in morning and afternoon winds.
Total	69 (65 acceptable)	63 desired. 1 HE-135-100 not collected, but had enough already.

4.2 Encounter Events

Figure 16 provides a summary of encounter events (loss/gain of horizontal, vertical, and overall well clear status). As indicated in Figure 16, 3 well clear violations did occur on 22 September (Tuesday). These should not have occurred as a vertical safety offset was employed. These could only occur if variability in aircraft altitudes resulted in loss of well clear in the vertical direction.

This did occur, as indicated by these well clear violations and by the vertical well clear violations that occurred on the first three test days. Further analysis regarding aircraft altitudes and loss of vertical well clear status is provided in the next section. For the three well clear violations, the degree of well clear violation was small as shown in Table 17. The first was only 10 ft from the vertical well clear boundary (and ~412 ft from the horizontal well clear boundary), the second was only ~90 ft from the horizontal well clear boundary (and 40 ft from the vertical well clear boundary), and the third was only 7 ft from the vertical well clear boundary (and ~297 ft from the horizontal well clear boundary). While these well clear violations were minor, future tests should be altered to minimize such violations.

Table 17. Summary data for 22 September 2020 encounters. All else is as in Table 9.

Scen. ID	Date	B. Time	E. Time	Intr./UAS Spd	H/V Cls. Spd	Status	CPA _h	CPA _v	CPA	WCV	h _{wc}	v _{wc}	d _{wc}
HE-0-100	09/22/2020	1838:26	1843:25	9999999/ 999999	9999999/ 9999999	0							
HE-135-100	09/22/2020	1845:26	1847:55	107.17/ 54.23	67.98/ 0.17	1	1588.01	240.00	1606.04	1	-411.99	-10.00	-10.00
HE-270-100	09/22/2020	1852:31	1854:28	90.95/ 50.93	106.46/ 0.96	1	1266.08	254.00	1291.31	2	-733.92	4.00	4.00
HE-45-100	09/22/2020	1857:21	1859:23	104.62/ 43.24	139.99/ -0.20	1	4541.88	267.00	4549.72	3	16882.47	-5.00	16882.47
HE-180-100	09/22/2020	1901:28	1903:20	9999999/ 999999	9999999/ 9999999	0							
HE-90-100	09/22/2020	1915:17	1917:52	104.95/ 53.33	109.87/ -5.36	1	1759.60	214.00	1772.57	1	-89.59	-40.00	-89.59
HE-180-100	09/22/2020	2013:00	2016:00	91.76/ 30.71	60.65/ 1.31	1	433.78	285.00	519.03	2	-1566.22	35.00	35.00
HE-135-100	09/22/2020	2018:50	2021:07	106.43/ 53.54	65.68/ 6.04	1	5446.68	302.00	5455.05	3	5374.66	-14.00	5374.66
HE-225-100	09/22/2020	2023:42	2025:40	92.52/ 47.96	69.79/ -0.29	1	2819.22	350.00	2840.86	0	819.22	100.00	825.30
HE-315-100	09/22/2020	2029:11	2031:15	86.62/ 54.69	130.88/ -0.82	1	1872.49	278.00	1893.01	2	-127.51	28.00	28.00
HE-0-100	09/22/2020	2037:50	2040:14	91.97/ 47.62	139.88/ 3.06	1	5558.02	318.00	5567.11	3	8741.10	-75.00	8741.10
HE-135-100	09/22/2020	2044:28	2046:15	107.11/ 52.60	77.22/ 1.89	1	4218.63	287.00	4228.38	0	2218.63	37.00	2218.94
HE-270-100	09/22/2020	2048:20	2050:15	88.69/ 48.29	98.45/ 1.81	1	1695.92	251.00	1714.40	1	-297.07	-7.00	-7.00
HE-45-100	09/22/2020	2052:39	2055:14	104.78/ 41.97	136.52/ -3.38	1	3510.73	271.00	3521.17	3	1997.49	-23.00	1997.49
HE-180-100	09/22/2020	2057:52	2100:02	92.08/ 33.43	56.81/ 0.73	1	2698.34	278.00	2712.62	3	4052.59	-60.00	4052.59
HE-90-100	09/22/2020	2105:42	2108:16	104.39/ 53.51	109.63/ 0.47	1	2895.35	350.00	2916.43	3	4492.53	-7.00	4492.53
HE-225-100	09/22/2020	2110:02	2112:32	88.52/ 41.80	67.84/ -0.16	1	2244.93	267.00	2260.75	3	7933.99	-65.00	7933.99
HE-90-100	09/22/2020	2118:20	2120:21	105.21/ 51.13	113.29/ -0.63	1	3089.03	336.00	3107.25	3	13190.02	-16.00	13190.02
HE-315-100	09/22/2020	2125:06	2126:42	89.46/ 52.65	133.07/ 5.77	1	4316.22	199.00	4320.80	3	2364.13	-53.00	2364.13
HE-0-100	09/22/2020	2134:47	2136:44	90.12/ 52.77	143.85/ 0.78	1	5938.30	236.00	5942.99	3	4042.07	-61.00	4042.07

Figure 16 shows that horizontal well clear violations occurred, but were relatively rare. For the September 2020 tests, a “late” threshold was used for triggering a maneuver. This threshold corresponds to that used in §2.2.4.3.4 of RTCA (2017), with the slight modification that the threshold distances were computed using a late threshold of 25 s rather than 20 s, resulting in the functional visual alert that is provided to the EO occurring 60 s from CPA_h.⁸ If average or early thresholds were used (90 s and 110 s from CPA_h), it is expected that no horizontal well clear violations (or well clear violations) would have occurred.

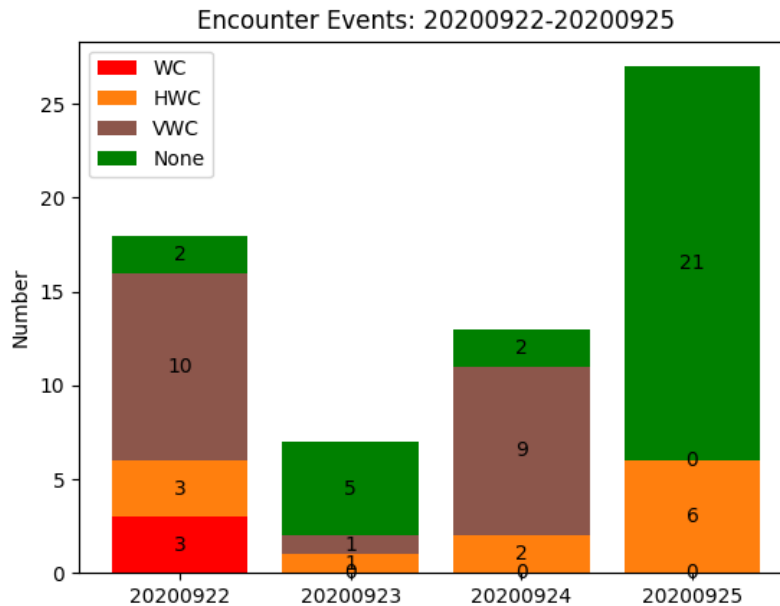


Figure 16. Encounter events for the September 2020 flight test encounters.

4.3 Vertical Separation Integrity

As indicated in the prior section, the vertical aircraft safety offset of 350 ft did not always ensure maintenance of vertical well clear, resulting in a few minor well clear violations. This is illustrated in Figure 17. As illustrated in Figure 17, MA altitude varied more than UA altitude, with UA altitude variability being roughly 1/3 to 1/2 of that of MA altitude variability during encounter OEPs. Inspection of the data (e.g., Table 10) indicated that the MA pilots were generally able to maintain their mean altitude within ± 50 ft, but not always. MA altitudes occasionally varied by ± 100 ft relative to mean values during OEPs (not shown). The biggest cause of loss of vertical well clear was lack of maintenance of mean altitude. For these tests, the planned MA altitude was 750 ft AGL and the planned UA altitude was 390 ft AGL. As shows in Figure 17, both aircraft operated at lower altitudes, with the decrease in the MA altitude being larger, resulting in vertical well clear (and well clear) violations.

⁸ A range ring was displayed on RangeVue™ to provide a visual cue to the EO that action was required. This range ring was changed for each encounter angle and intruder speed because variations in these variables resulted in different closure rates.

MA altitude integrity performance varied. As shown in Figure 18, performance on 25 September 2020 was much better. Given these results, it is recommended that future tests utilize a 400 ft vertical safety offset and that the altitude of the MA be monitored to ensure that its mean altitude is close to that intended.

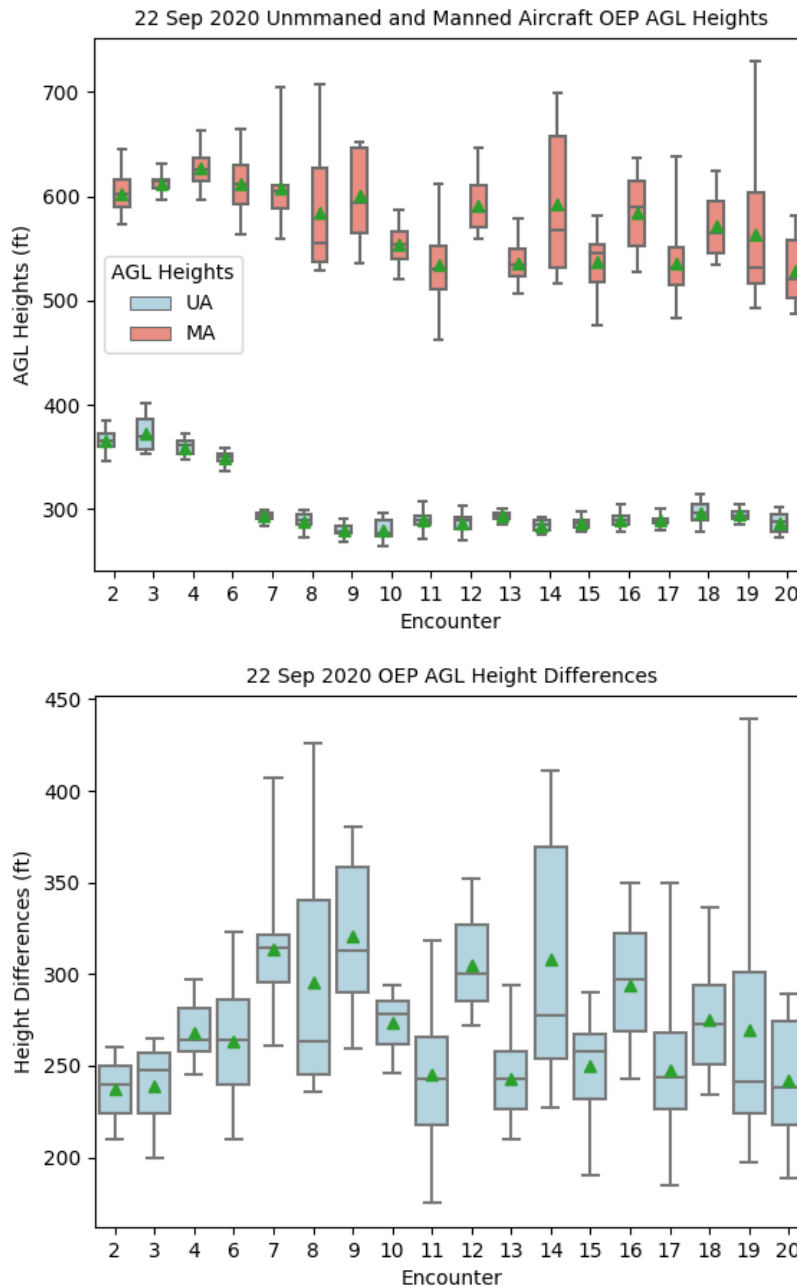


Figure 17. Box-and-whisker plots of aircraft AGL altitudes (top) and aircraft altitude differences (bottom) for 22 September 2020. Box edges indicate the lower and upper quartiles, the lines within

the boxes indicate medians, the green triangles indicate means, and the whiskers encapsulate the full ranges of values.

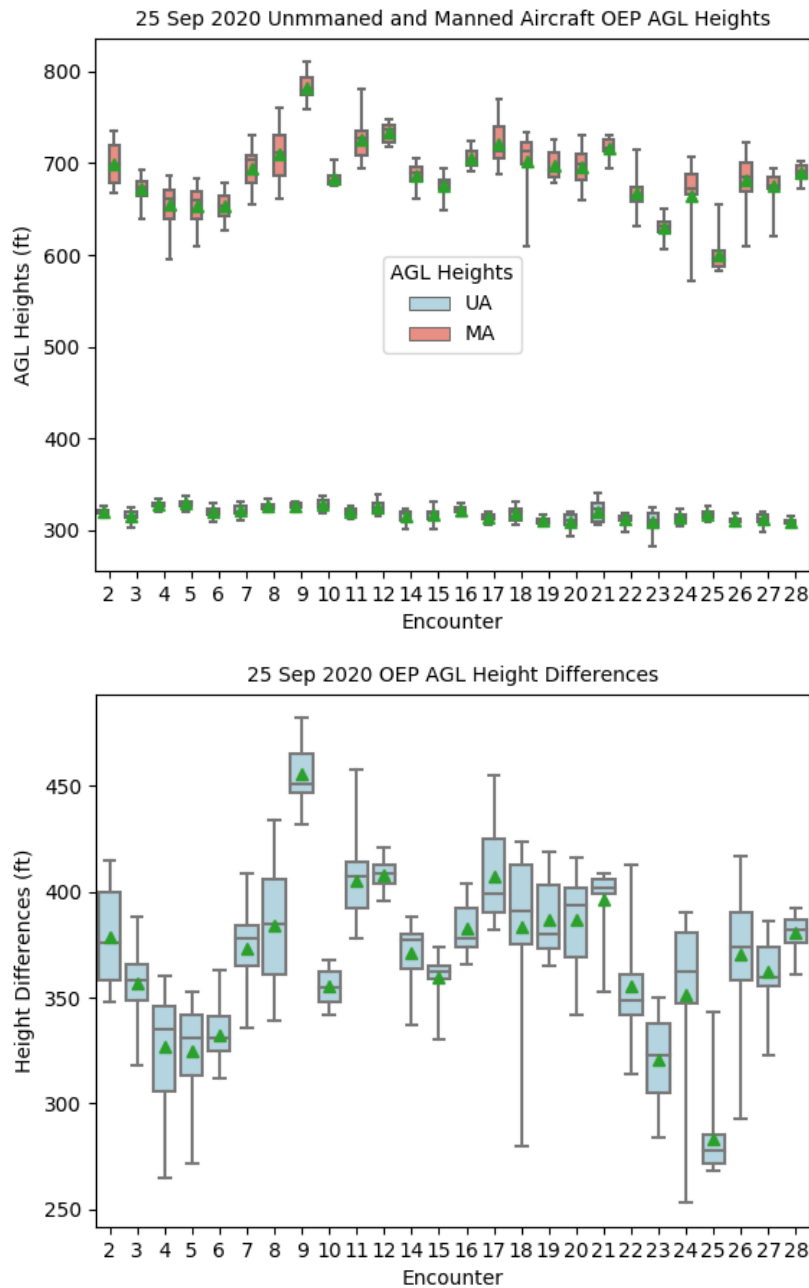


Figure 18. As in Figure 17, but for 25 September 2020.

4.4 Example Encounters

Example encounters are examined to develop an understanding of overall encounter characteristics. These include an encounter characterized by a vertical well clear violation, an encounter characterized by a horizontal well clear violation, and an encounter in which no violation occurred.

An encounter characterized by a vertical well clear violation is illustrated in Figure 19. As illustrated, the vertical well clear violation occurs early in the OEP, and it appears as if the MA was adjusting altitude at that time after completing a turn to initiate the encounter (as indicated by the beginning of the inbound segment for the MA). While some of the vertical well clear violations occurred as a result of the MA coming out of a turn to initiate an encounter (or as the MA enters a turn to set up for the next encounter), the majority of the vertical well clear violations shown in Figure 16 were not associated with such maneuvers. Examination of the encounters indicates that 3 of the 20 identified vertical well clear violations were associated with MA turns. Thus, the primary drivers of vertical well clear violations were mean MA altitudes that were too low relative to the planned test altitude and variations in MA altitudes.

An encounter characterized by a horizontal well clear violation is illustrated in Figure 20. As indicated in this figure (cf. the separation timeline), the chosen maneuver initially resulted in a higher closure rate between the aircraft. This is driven by two factors. The first is the path of the MA is to the west of that of the UA (prior to maneuver). Thus, the turn towards the west for the UA results in increased closure between the aircraft. The second factor is that with such a maneuver the closure in the direction of travel of the MA overwhelms the separation realized in the direction of travel of the UA for a period of time after the UA maneuvers. This is illustrated using (13). If the separation between the two aircraft is increasing with time, this quantity is positive. For simplicity, the scenario where the MA is travelling due south (at the 100 kt test speed) and the UA travels due west (at its presumed cruise speed of 45 kts) is considered. In this scenario, the origin is the starting point of the UA, which is due south of the MA an initial distance of 3500 ft (the approximate horizontal separation of the aircraft in Figure 20 at the time of maneuver initiation). Thus, the parameters in (13) for this scenario are:

- $u_{MA} = 0$ kts
- $u_{UA} = -45$ kts
- $x_{MA0} = 0$
- $x_{UA0} = 0$
- $v_{MA} = -100$ kts
- $v_{UA} = 0$ kts
- $y_{MA0} = 3500$ ft
- $y_{UA0} = 0$ ft

For these assumptions (eliminating the terms that are 0), solving for the time t when the square of the horizontal aircraft separation increases produces

$$t > \frac{-v_{MA} y_{MA0}}{u_{UA}^2 + v_{MA}^2}. \quad (33)$$

For these values, $t = 17.24$ s, at which point $CPA_h = 1436.28$ ft. The actual CPA_h is smaller than this, which likely results from the MA path being to the west of that of the UA (prior to UA maneuver) and to the variations in the actual encounter relative to assumed values (e.g., UA speed). Values of horizontal aircraft separation for this scenario have been computed as a function of time and horizontal aircraft closure rates have been computed from those values. One-half second into the UA travelling westward the horizontal closure rate is estimated to be 167.92 ft s^{-1} , which is significantly larger than the 92.83 ft s^{-1} horizontal aircraft closure rate that occurs when the MA is

directly overtaking the UA (180° encounter geometry). For this scenario, the closure rate falls below the overtaking closure rate ~14.22 s after the UA begins travelling west. This highlights a fundamental challenge associated with DAA—aircraft separation typically decreases for a period after maneuver initiation and closure rates can increase after maneuver initiation. Both of these must be considered to ensure maintenance of well clear.

Figure 21 illustrates an encounter for which no well clear violation occurred. The separation timeline shows a period after maneuver initiation during which the horizontal closure rate increased. Relative to Figure 20, however, this increase occurred for a shorter period of time and was less pronounced.

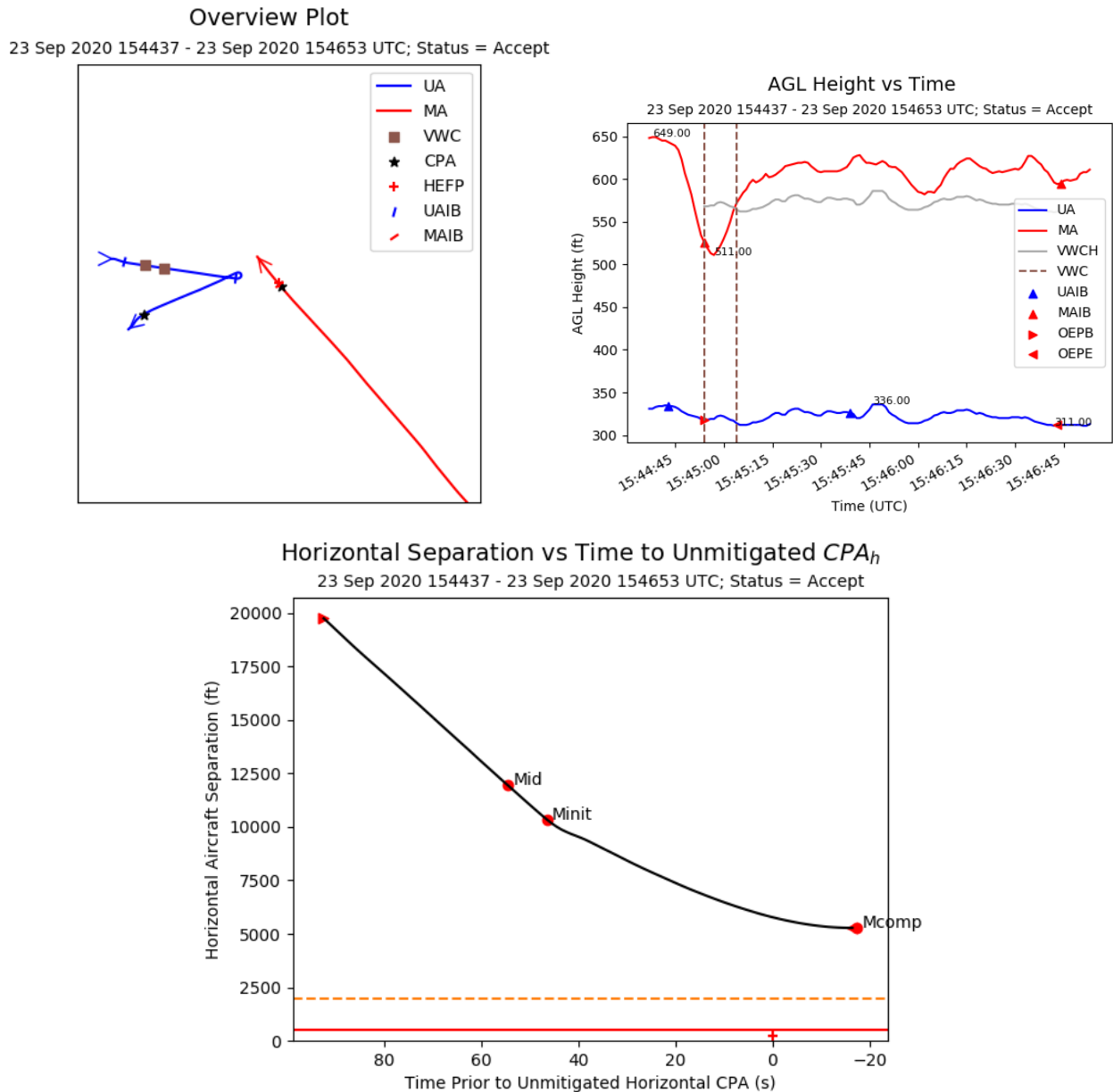
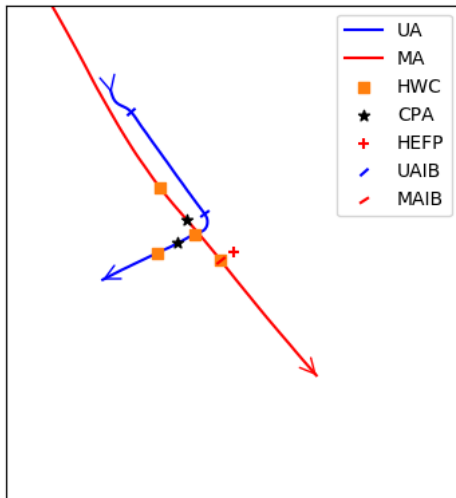


Figure 19. Illustration of the 154437-154653 UTC 23 September 2020 encounter. Upper left provides a plan view, with the UA flight path in blue, MA flight path in red, the period of vertical well clear violation

indicated by brown boxes superimposed on the UA flight path (well clear and horizontal well clear are indicated by red and orange boxes, respectively), CPA indicated with a black star symbol, the HEFP indicated with a red plus symbol, and the inbound portions of flight indicated by blue (UA) and red (MA) dashes. Upper right provides a plot of AGL altitudes (relative to HEFP altitude), with the UA altitudes in blue, the MA altitudes in red, the MA altitudes needed to maintain vertical well clear in dark grey, the times of vertical well clear violation indicated by dashed down lines (well clear and horizontal well clear are indicated by dashed red and orange lines, respectively), the UA inbound portion indicated by blue triangles, the MA inbound portion indicated by red triangles, and the OEP beginning and end indicated by rotated red triangles. Bottom is the separation timeline, with the horizontal well clear boundary indicated by the orange dashed line (colored red if a well clear violation occurs), the horizontal NMAC boundary indicated by the solid red line, unmitigated CPA_h indicated by the red plus symbol, the time when both aircraft are inbound indicated with a rotated red triangle (left side of plot), the OEP end indicated with a rotated red triangle (right side of plot), and labels indicating the following: Dfst=First Detection, Testblsh = Track Establishment, Ecaut = Caution, Ewarn = Warning, Mid = Maneuver Identification, Minit = Maneuver Initiation, and Mcomp = Maneuver Completion.

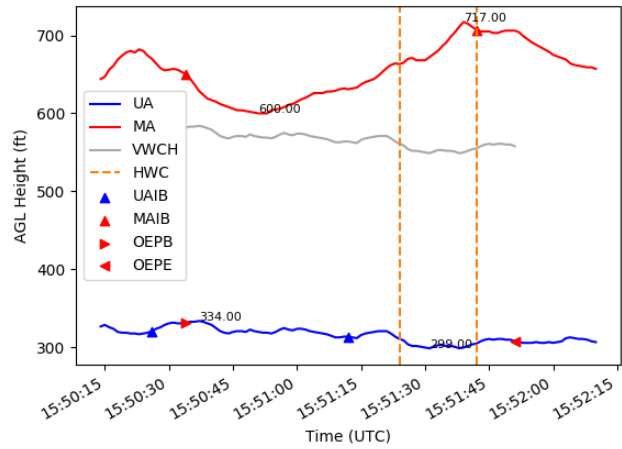
Overview Plot

23 Sep 2020 155014 - 23 Sep 2020 155210 UTC; Status = Accept



AGL Height vs Time

23 Sep 2020 155014 - 23 Sep 2020 155210 UTC; Status = Accept



Horizontal Separation vs Time to Unmitigated CPA_h

23 Sep 2020 155014 - 23 Sep 2020 155210 UTC; Status = Accept

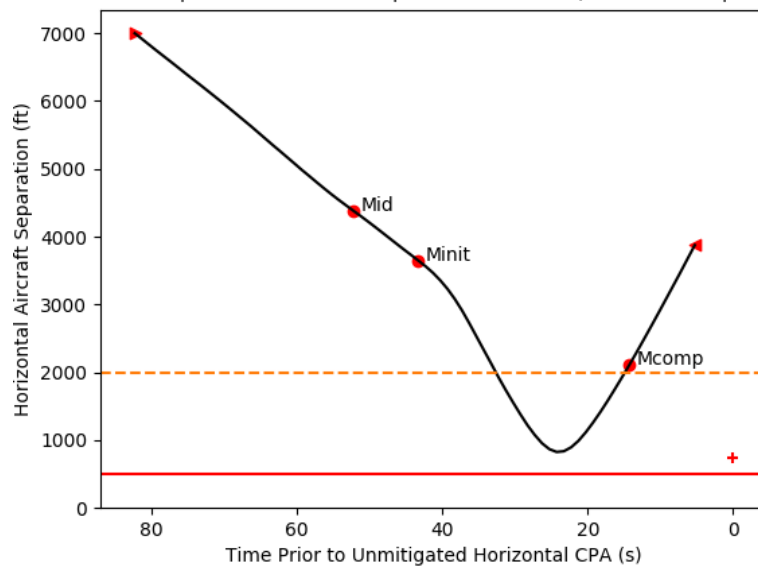


Figure 20. As in Figure 19, but for the 155014-155210 UTC 23 September 2020 encounter.

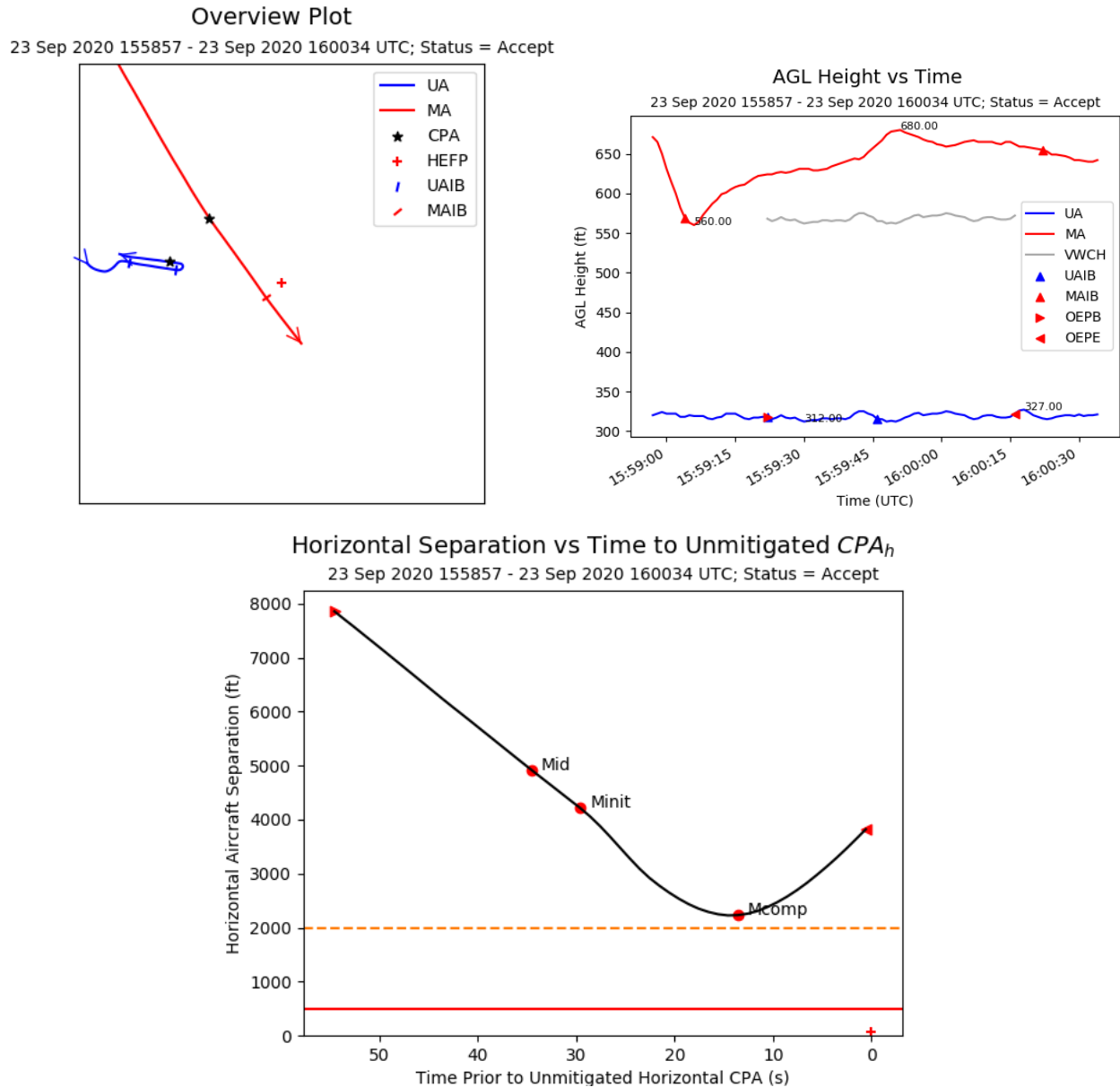


Figure 21. As in Figure 19, but for the 155857-160034 UTC 23 September 2020 encounter.

4.5 Sample Risk Ratio and Sample Risk Ratio Uncertainty

LR_{ch} values for the 80 and 100 kt intruder speed tests are provided in Figure 22. This figure also provides uncertainties regarding LR_{ch} derived using the non-homogeneous assumption. Uncertainties for the 80 kt intruder speed tests are not provided owing to not having enough samples for each encounter geometry (at least 3 samples are required).

For the 80 kt intruder speed tests, $LR_{ch} = 0.19$, and for the 100 kt intruder speed tests, $LR_{ch} = 0.26$ with an uncertainty window of 0.13-0.34. With the non-homogeneous approach, the uncertainty window is not necessarily centered on the estimated value. It is noted that Figure 21, especially the 100 kt intruder speed tests (more data points and difference in performance for 0° - 135°

encounter geometries and 180°-315° encounter geometries), indicates that the non-homogeneous assumption regarding CPA_h is warranted/supported.

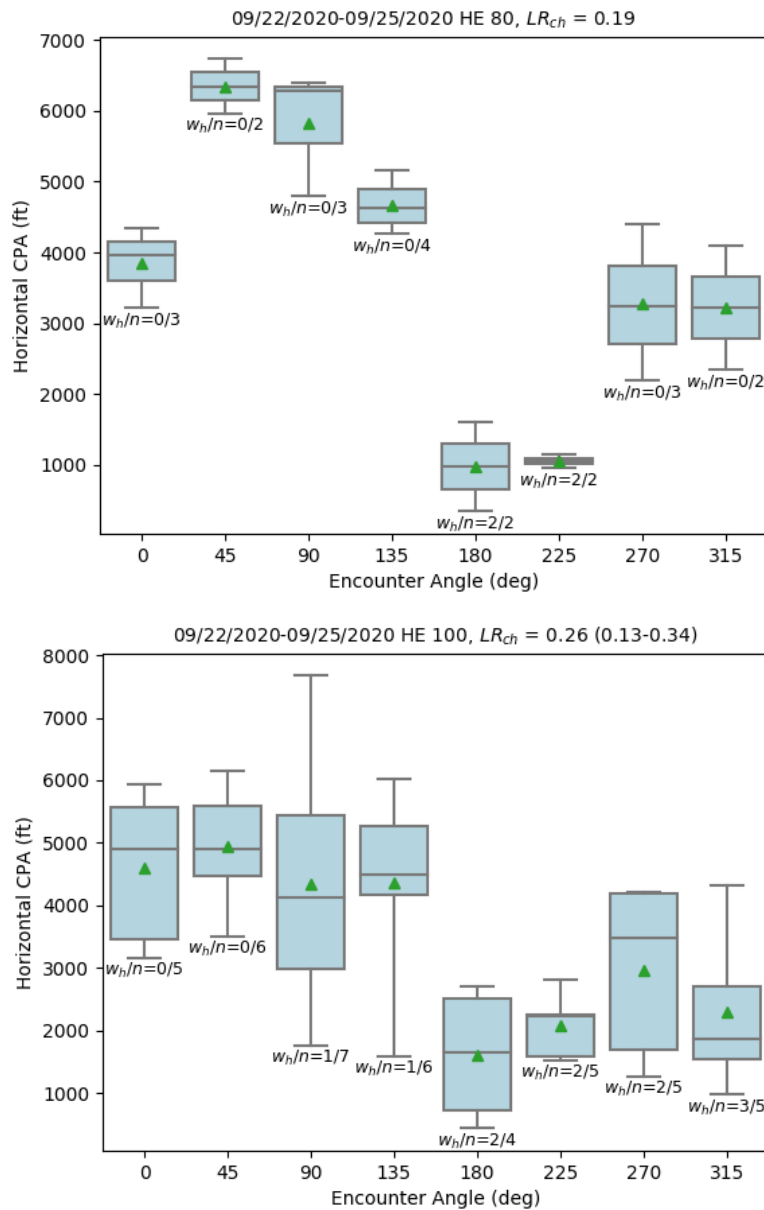


Figure 22. Box and whisker plots of CPA_h for the encounter geometries for each intruder speed. Top figure is for 80 kt intruder speed tests and bottom figure is for 100 kt intruder speed tests. The box and whisker features are as in Figure 17. The symbol w_n indicates the number of horizontal well clear violations (including well clear violations) and the symbol n indicates the total number of encounters for each encounter

geometry. LR_{ch} values are provided in the figure title, with the corresponding uncertainty window in parentheses.

The first homogeneous approach, the binomial proportion confidence interval approach, produced $LR_{ch} = 0.204 \pm 0.085$ (0.119-0.289) for the 80 kt intruder speed tests and $LR_{ch} = 0.261 \pm 0.066$ (0.195-0.327) for the 100 kt intruder speed tests.

Results for the second homogeneous approach are illustrated in Figure 23. As indicated in Figure 23, for the 80 kt intruder speed tests $LR_{ch} = 0.19$ with an uncertainty window of 0.096-0.287, and for the 100 kt intruder speed tests $LR_{ch} = 0.256$ with an uncertainty window of 0.159-0.298.

A comparison of LR_{ch} values and uncertainty windows for the three methods is provided in Table 18. As indicated in this Table, the non-homogeneous uncertainty window is the widest (of the three methods for 100 kts). For 80 kts, the two homogeneous methods produce very similar results. For 100 kts, the uncertainty window values for the 2nd homogeneous method are lower than those for the first homogeneous method.

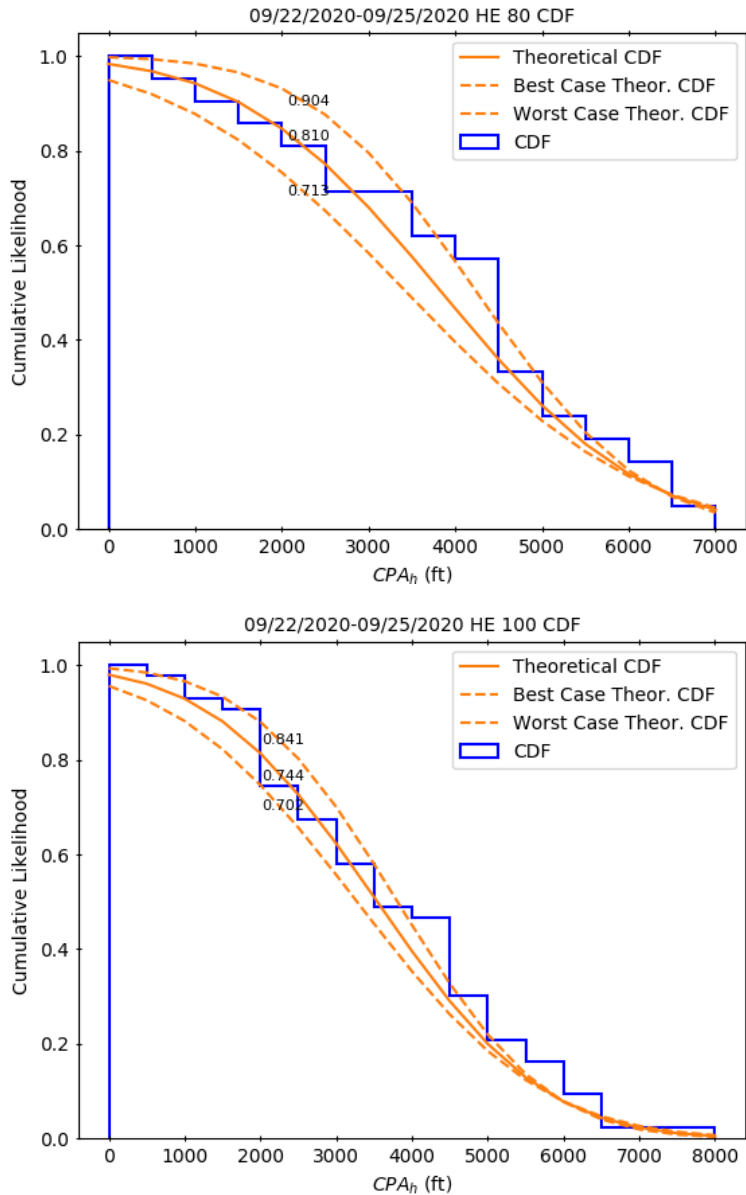


Figure 23. Cumulative Density Functions (CDFs) of CPA_h for the encounter geometries for each intruder speed. Top figure is for 80 kt intruder speed tests and bottom figure is for 100 kt intruder speed tests. The solid blue line indicates the CDF directly from the data, the solid orange line indicates the CDF derived from statistical properties of the data (mean and standard deviation), the dashed orange lines are the best- and worst-case CDFs (top and bottom, respectively), and numbers indicate the likelihood CPA_h ≥ 2000 ft for the respective distribution.

Table 18. Comparison of LR_{ch} values and uncertainty windows. Values are organized according to intruder speed, with values at each speed encompassing horizontal encounter geometries ranging from 0° - 360° degrees sampled every 45°

Method	Lower Uncertainty Window Value	LR_{ch}	Upper Uncertainty Window Value
80 kts Intruder Speed Tests			

Non-homogeneous		0.19	
1 st homogeneous (binomial proportion confidence interval)	0.119	0.204	0.289
2 nd homogeneous (Normal distribution)	0.096	0.19	0.287

100 kts Intruder Speed Tests			

Non-homogeneous	0.13	0.26	0.34
1 st homogeneous (binomial proportion confidence interval)	0.195	0.261	0.327
2 nd homogeneous (Normal distribution)	0.159	0.256	0.298

5 CONCLUSIONS

5.1 Lessons Learned

Lessons learned from this round of flight tests include:

- Failures associated with testing occur, including ones experienced during this round of flight tests:
 - The wired connection from the radar to the Electronic Observer Trailer failed the week before testing. This was repaired the Friday prior to testing.
 - The LTE connection dropped at the Electronic Observer Trailer. This interrupted communications and connectivity for DCAPS.
 - Resulted in one encounter being unacceptable.
 - The Command Center Trailer generator ran out of gas.
 - The Uninterruptable Power Supply (UPS) kicked in.
 - Communications were lost—Zoom™.
- Detection challenges occur
 - ADS-B drop-outs did occur and seemed to be focused on a certain location.
 - Primary tracks (radar) did not always arise for aircraft taking-off and landing at the airport.
 - The clutter filter is believed to be the cause of this.
- Display glitches can occur
 - Occasionally the locations of UA and MA did not (seemingly) update on RangeVue™
 - This resulted in aircraft positions “jumping”

5.2 Utilization in ASTM WK62669 DAA Test Methods Task Group

The results from this round of testing are being utilized in the ASTM WK62669 DAA Test Methods Task Group. Results have been presented to the overall group, and are being utilized in a subgroup that is focused on flight testing. Topics that are being leveraged include:

- Flight test approach (geometric)
- Data elements (e.g., DTEM)
- Sample risk ratio uncertainty estimation

One of the major challenges faced by this group is simulation validation. Topics that are being leveraged to propose a path forward include risk ratio decomposition (§2.1.2.3) and statistical methods utilized to evaluate uncertainty (§3.1.2.2).

This working group has identified one path for demonstrating DAA system compliance that involves system simulation that is validated using flight test results. In that approach, simulation results are compared to flight test results, with adjustments made to the simulation framework as indicated by the flight tests. The most direct comparison is of the set of simulated encounters that corresponds with the set executed during flight tests. Once correspondence is achieved—something that the committee is still defining—the full set of simulated encounters can be used with significant confidence that they represent real-world performance.

5.3 Future Work

Numerous topics should be evaluated further. These include:

- Inclusion of other variations in flight tests (curved trajectories, climb/descend-into encounters, etc.).
- Ensuring safety while including other variations in flight tests.
- Impacts of expanding the number of encounters for an encounter geometry (especially impacts on uncertainties).
- Environmental impacts—especially impacts of the wind on the ability to maintain well clear status. It is expected that a UA maneuver into the wind will increase the risk ratio and decrease CPA values.
- Additional visualization techniques. An interactive 3D visualization approach has been suggested as an excellent way to interrogate/understand individual encounters.

5.4 Summary

A summary of the test plan for this test event is provided. This includes:

- Background Information: Standards efforts and encounter characteristics
- Objectives
- Personnel
- DAA system
- Aircraft
- Test locations
- Test dates and schedule
- Test conditions
- Test cards
- Data collection and management

This test plan leverages a geometric approach to gathering data, in which potential encounter geometries are varied. It also includes limited evaluation of speed variations. At present, horizontal encounters are evaluated, as development of safe means for testing descend- and climb-into encounters are currently being developed. Pragmatic drivers, including time and cost, result in a subset of the total number of possible encounters being evaluated. A vertical aircraft altitude offset of 350 ft was used during these tests to enable maintenance of well clear status during the tests.

Given that these tests utilized a DAA system that leverages a ground-based radar and ADS-B data, the full 360° of potential horizontal encounter geometries is spanned. Horizontal encounter geometries are evaluated at 45° increments (0°, 45°, 90°, 135°, 180°, 225°, 270°, and 315°). Two sets of intruder speeds are utilized—100 kts and 80 kts. The test plan involved executing 5 encounters for each geometry for the 100 kt intruder speed and 2 encounters for the 80 kt intruder speed. Except for the 180° encounter geometry at 100 kt intruder speed, for which 4 successful encounters were executed, at least the number of desired encounters were completed for each geometry and intruder speed. It is noted that use of a DAA system that utilized ADS-B data (and a ground-based radar data) resulted in the challenge of maintaining well-clear being focused on the EM steps of DTEM. Disregarding data drop-outs, maintaining well clear was driven by evaluating and maneuvering early enough in the encounters. Such a system has very limited detection range dependency, which results in less sensitivity to closure rates/intruder speeds.

Metrics were developed for individual encounters and for the entire test campaign. For individual encounters, encounter events are defined as well clear violations, horizontal well clear violations, and vertical well clear violations. Encounter descriptors were developed to identify important segments of encounters. These include the period when the UA and MA are inbound to the HEFP, when the UA maneuvers, and the OEP, which is the period within an encounter when the two aircraft are deemed to be interacting. Distance metrics include the distance to the well clear boundary d_{wc} , which provides information regarding how well well-clear was maintained or how severely well-clear was violated, and CPA, which is decomposed into horizontal and vertical components. Metrics associated with the Detect, Track, Evaluate, and Maneuver (DTEM) steps are also provided. These are provided as tabular data for each step.

Campaign metrics include sample risk ratio and sample risk ratio uncertainty. Sample risk ratio is easily computed given that each acceptable encounter is considered to result in a well clear violation (in reality a horizontal well clear violation owing to the use of a vertical aircraft offset for safety). Sample risk ratio uncertainty estimates are provided using three approaches, all of which utilize CPA_h values. The first, and most complicated, assumes that statistical properties of CPA_h can vary with encounter geometry, while the other two approaches assume homogeneity of CPA_h values with respect to encounter geometry.

The team developed software to enable rapid processing of test data. Python is used owing to its enablement of rapid code development and its rich set of modules for analysis and visualization. Two primary code sets comprise the software—'ByDay' software used to analyze encounters executed in single day of flight testing and 'Campaign' software used to produce overall campaign results.

Visualization tools enable comprehension of encounter characteristics. Tools developed for examining individual encounters include a plan-view plot that shows aircraft tracks and metrics,

XY plots that show aircraft altitudes and metrics, and a separation timeline that shows aircraft separation as a function of time with overlaid encounter metrics. Other visualization tools developed include box and whisker plots to understand statistical characteristics of data (e.g., aircraft altitudes, CPA_h , etc.).

Despite use of a vertical safety offset, 3 minor well clear violations did occur during testing. Analysis of aircraft altitudes shows that MA altitudes varied more significantly than UA altitudes. However, the primary cause of loss of desired vertical separation was failure to maintain the desired mean MA altitude. Thus, it is recommended that future tests utilize a 400 ft vertical safety offset and that the altitude of the MA be monitored to ensure that its mean altitude is close to that intended.

Horizontal well clear violations did occur, but were relatively rare. This is underscored by the sample risk ratio results discussed subsequently.

Examination of encounters revealed an interesting scenario where a seemingly well-chosen maneuver resulted in a temporary increase in aircraft closure rate. In this situation the MA was overtaking the UA from behind (180° encounter geometry) and the UA maneuvered in an orthogonal direction. The cause of the increased closure rate is validated using a mathematical model. Such impacts of maneuvering need to be considered when determining alerting boundaries to ensure maintenance of well clear.

The sample risk ratio for the 100 kt intruder tests is 0.26 and for the 80 kt intruder tests is 0.19. The lower sample risk ratio for the 80 kt intruder tests aligns with expectations given the smaller difference between MA and UA speeds. That accuracy of this value, however, is in question given the small number of samples/tests for that speed.

Sample risk ratio uncertainties for both intruder speeds are generally less than 0.1, with less confidence in values for the 80 kt intruder tests given the relatively low number of encounters for that speed. These uncertainties, especially for the 100 kt intruder speed, indicate that the encounter test set is viable for providing guidance regarding conformance with the performance standard.

These results must be placed in context with the broader set of possible encounters, the breadth of which can be evaluated through simulation. Moreover, the metrics that are developed herein for the major stages of DAA, which were developed through the need for information regarding how the system is performing and qualified by pragmatic considerations (e.g., timing challenges associated with data collection), provide useful information regarding these major stages (and are being considered by the ASTM WK62669 DAA Test Methods Task Group). Finally, methods developed for analyzing encounters, which include visualization techniques and summary metrics, enable understanding of encounter characteristics. This includes the situation wherein aircraft closure rates increase for a period of time after maneuver initiation.

Bibliography

- Askelson, et al., 2017: Small UAS Detect and Avoid Requirements Necessary for Limited Beyond Visual Line of Sight (BVLOS) Operations. USDOT FAA (ASSURE), 516 pp.
- ASTM 2020: Standard Specification for Detect and Avoid System Performance Requirements. F3442/F3442-20, 22 pp.
- Barr, D. R., and E. T. Sherrill, 1999: Mean and variance of Truncated Normal distributions. *The American Statistician*, **53**(4), 357-361.
- Burkart, J., 2014: The Truncated Normal Distribution. 35 pp., https://people.sc.fsu.edu/~jburkardt/presentations/truncated_normal.pdf.
- C Speed, 2021: Lightwave Radar. Accessed 12 April 2021, <http://www.cspeed.com/radar>.
- Deaton, J. L., and R. J. Hansman, 2019: Investigating Collision Avoidance for Small UAS Using Cooperative Surveillance and ACAS X. ICAT-2019-06. 126 pp.
- D'Agostino, R. B., 1971: An omnibus test of normality for moderate and large sample size. *Biometrika*, **58**, 341-348.
- D'Agostino, R., and E. S. Pearson, 1973: Tests for departure from normality. Empirical results for the distributions of b_2 and $\sqrt{b_1}$. *Biometrika*, **60**, 613-622.
- e-CFR, 2021a: Part 135— Operating Requirements: Commuter and on Demand Operations and Rules Governing Persons on Board Such Aircraft. Accessed 15 September 2021, <https://www.ecfr.gov/current/title-14/chapter-I/subchapter-G/part-135?toc=1>.
- e-CFR, 2021b: Part 107—Small Unmanned Aircraft Systems. Accessed 21 April 2021, <https://www.ecfr.gov/cgi-bin/text-idx?node=pt14.2.107&rgn=div5>.
- Edwards, M. W., M. J. Kochenderfer, J. K. Kuchar, and L. P. Espindle, 2009: Encounter Models for Unconventional Aircraft Version 1.0. Project Report ATC-348, 84 pp.
- FAA 2021: Satellite Navigation-Wide Area Augmentation System (WAAS). Accessed 6 June 2021, https://www.faa.gov/about/office_org/headquarters_offices/ato/service_units/techops/nav_services/gnss/waas/.
- FAA William J. Hughes Technical Center, 2020: Wide Area Augmentation System Performance Analysis Report—October 2020. Report #74, 197 pp., https://www.nstb.tc.faa.gov/reports/2020_Q3_FAA_WAAS_PAN_Report_74_v1.0.pdf.
- Griffith, J. D., M. W. M. Edwards, R. M. C. Mirafior, and A. J. Weinert, 2013: Due Regard Encounter Model Version 1.0. Project Report ATC-397, 56 pp.
- Harris, 2016: Symphony® RangVue™, 2 pp., http://www.symphonycdm.com/Pages/sites/default/files/products/pdf/RangeVueDataSet_web.pdf.

- ICAO, 2014: Aeronautical Communications: Volume IV—Surveillance and Collision Avoidance Systems (Annex 10 to the Convention on International Civil Aviation). 216 pp.
- L3Harris, 2021: ADS-B Xtend™ for Airports. Accessed 12 April 2021, <https://www.l3harris.com/all-capabilities/ads-b-xtend-airports>.
- Newcombe, R. G., 1998: Two-sided confidence intervals for the single proportion: Comparison of seven methods. *Stats. in Medicine*, **17**, 857-872.
- Qstarz, 2021: BT-Q1000XT. Accessed 6 June 2021, <http://www.qstarz.com/Products/GPS%20Products/BT-Q1000XT-F.htm>.
- RTCA, 2017: Minimum Operational Performance Standards (MOPS) for Detect and Avoid (DAA) Systems. RTCA, Inc., 838 pp.
- Schäfer, M., M. Strohmeier, V. Lenders, I. Martinovic, and M. Wilhelm, 2014: Bringing up OpenSky: A large-scale ADS-B sensor network for research. *IPSN-14 Proc. 13th Int. Symp. on Inf. Proc. in Sensor Networks*, 83-94.
- Stones Mobile Radio, 2021: Stonecast. Accessed 19 April 2021, <https://www.stonesmobileradio.com/products/stonecast-tower-network/>.
- Taylor, J. R., 1996: *An Introduction to Error Analysis*. 2nd Ed., Univ. of Science Books, 327 pp.
- Underhill, N. K., E. P. Harkleroad, R. E. Guendel, A. J. Weinert, D. E. Maki, and M. W. M. Edwards, 2018: Correlated Encounter Model for Cooperative Aircraft in the National Airspace System Version 2.0. Project Report ATC-440, 138 pp.
- USDOT, 2021: Satellite Navigation – Wide Area Augmentation System (WAAS). Accessed 6 June 2021. https://www.faa.gov/about/office_org/headquarters_offices/ato/service_units/techops/nav_services/gnss/waas.
- Van Rossum, G., and F. L. Drake, 2009: *Python 3 Reference Manual*. Scotts Valley, CA., 242 pp.
- Virtanen, P., R. Gommers, T. E. Oliphant, M. Haberland, T. Reddy, D. Cournapeau, E. Burovski, P. Peterson, W. Weckesser, J. Bright, S. J. van der Walt, M. Brett, J. Wilson, K. J. Millman, N. Mayorov, A. R. J. Nelson, E. Jones, R. Kern, E. Larson, C. J. Carey, Í. Polat, Y. Feng, E. W. Moore, J. VanderPlas, D. Laxalde, J. Perktold, R. Cimrman, I. Henriksen, E. A. Quintero, C. R. Harris, A. M. Archibald, A. H. Ribeiro, F. Pedregosa, P. van Mulbregt, and SciPy 1.0 Contributors, 2020: SciPy 1.0: Fundamental algorithms for scientific computing in Python. *Nature Methods*, **17**(3), 261-272.
- Weinert, A., and G. Barrera, 2020: A review of low altitude manned aviation operations. Preprints 2020, 2020070522, doi: 10.20944/preprints202007.0522.v1, <https://www.preprints.org/manuscript/202007.0522/v1>.
- Weinert, A. J., E. P. Harkleroad, J. D. Griffith, M. W. Edwards, and M. J. Kochenderfer, 2013: Uncorrelated Encounter Model of the National Airspace System Version 2.0. Project Report ATC-404, 93 pp.

- Weinert, A, S. Campbell, A. Vela, D. Schuldt, and J. Kurucar, 2018: Well-clear recommendation for small unmanned aircraft systems based on unmitigated collision risk. *J. Air Transp.*, **26**, 113-122.
- Weinert, A., N. Underhill, and A. Wicks, 2019: Developing a low altitude manned encounter model using ADS-B observations. *IEEE Aerospace Conference 2019*, Big Sky, MT, <https://ieeexplore.ieee.org/document/8741848>.
- Wikipedia, 2021: Binomial Proportion Confidence Interval. Cited 2021, https://en.wikipedia.org/wiki/Binomial_proportion_confidence_interval#Wilson_score_interval_with_continuity_correction.
- Wilson, E. B., 1927: Probable inference, the law of succession, and statistical inference. *J. Amer. Statistical Assoc.*, **22**(158), 209-212.

Appendix A: High-Level Overview of Test Process

Tests are based upon test scenarios, which are labelled according to encounter geometry and intruder speed. The encounter scenarios are indicated using the following nomenclature:

- HE_0__120: Horizontal Encounter at a 0° relative intruder course angle with the intruder flying at 120 kts.
- CE_0_45__120: Climb-into Encounter at 0° horizontal relative intruder course angle with the intruder flying at 120 kts.
- DE_0_-45__120: Descend-into Encounter at 0° horizontal relative intruder course angle and -45° intruder elevation with the intruder flying at 120 kts.

Test roles include:

- Flight test director: The person who is responsible for overall coordination of encounters, including declaration of checkpoints.
- Unmanned Aircraft (UA) PIC: Person responsible for operation of the UA.
- Manned Aircraft (MA; intruder) pilot: Person responsible for operation of the MA/intruder.
- Visual Observer (VO): Assists UA PIC with see and avoid function.
- Data collector: A person who helps collect data (e.g., records times of events).
- Electronic Observer: Monitors a display system that provides a visualization of the test range, including real-time locations of ownship, intruder, and the HEFP (Horizontal Encounter Focal Point).
- Tech support: Keeps technology functioning during test. This maybe a combination of industry support and ASSURE A18 performers.

Test Waypoints are:

- Horizontal Encounter Focal Point (HEFP): For horizontal encounter scenarios, the horizontal location at which both aircraft would arrive at the same time if neither maneuvered and if a vertical safety offset was not employed.
- Vertical Encounter Focal Point (VEFP): For vertical encounter scenarios, the vertical location at which both aircraft would arrive at the same time if neither maneuvered and if a horizontal safety offset was not employed.

Test Checkpoints are:

- Unmanned aircraft Setup Exit (USE): The time at which the UA exits its orbit to proceed to scenario start.
- Scenario Start (SS): This is declared by the flight test director once the time for arrival at the HEFP for both aircraft is within tolerance.
- Encounter Initiation (EI): The time at which the flight test director declares that the encounter has begun (based upon criteria provided below). A data collector records this.
- First Detection (FD): The time at which the DAA system first detects the intruder. A data collector records this.
- Track Establishment (TE): The time at which a track for the intruder is established. This is recorded either automatically using software or by a data collector.
- Maneuver Initiation (MI): The time of ownship maneuver initiation. This is recorded either automatically using software or by a data collector.

- Encounter End (EE): The time at which the flight test director declares that the encounter has ended. A data collector records this. After this, both aircraft move to set up (S) the next encounter.

The testing process for a horizontal encounter is illustrated in Figure A1. The sequence of events is described in the HE_0 Test Cards.

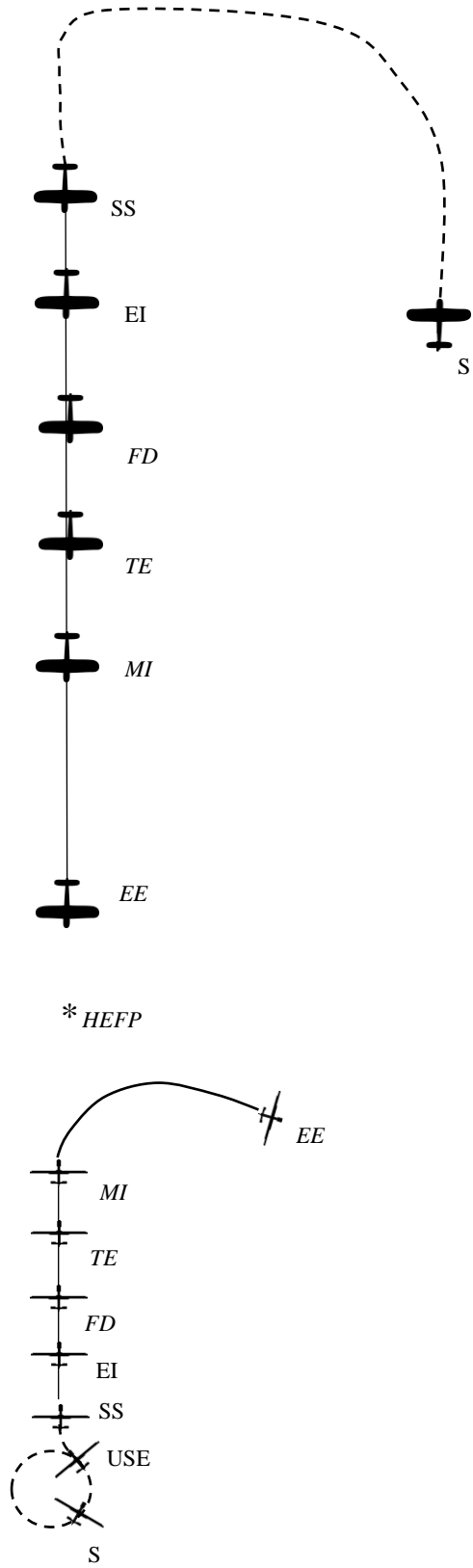
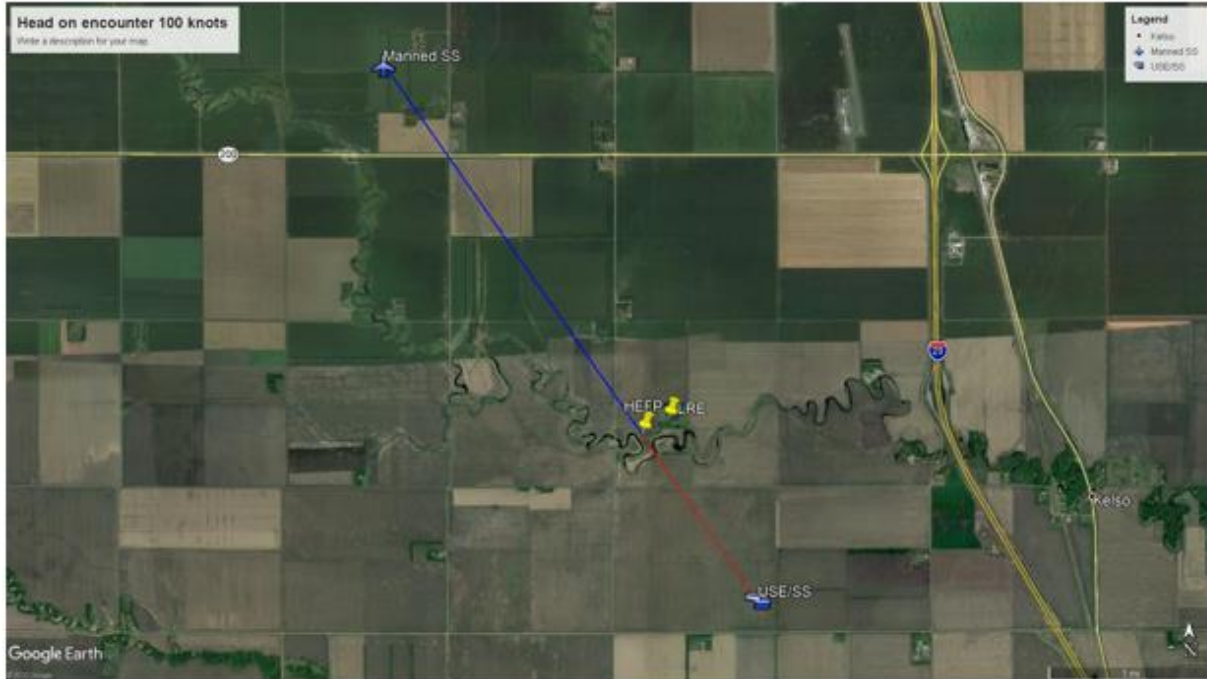


Figure A1. Illustration for an HE_0 scenario.

**Appendix B: Test Cards/Scripts for UND/NPUASTS 21-25
September 2020 Tests**

A total of 48 cards (8 encounter angles x 2 intruder speeds x 3 roles) support this test campaign. For clarity, different cards are used for the roles of flight test director (Master/overall), the intruder, and the UAS. Example test cards/scripts for HE_0__100 are provided in the following pages; the full set of scripts/cards is not provided herein for brevity.

Overall Test Card



Flight Card #	A18-ND-Master-HE-0-100
Date/Time	
Objective	
Description	Manned aircraft and UAS encounters are conducted at the indicated cruise speeds. A vertical offset of 300' used to provide safety margin.
UAS Platform	FX 20
UAS Altitude	390 ft
UAS Speed	45 knots
Intruder	C150
Intruder Altitude	750 ft
Intruder Speed	100 knots
Location	47.328505, -97.087696. Lovas Farmstead.
GCS	Mission Planner



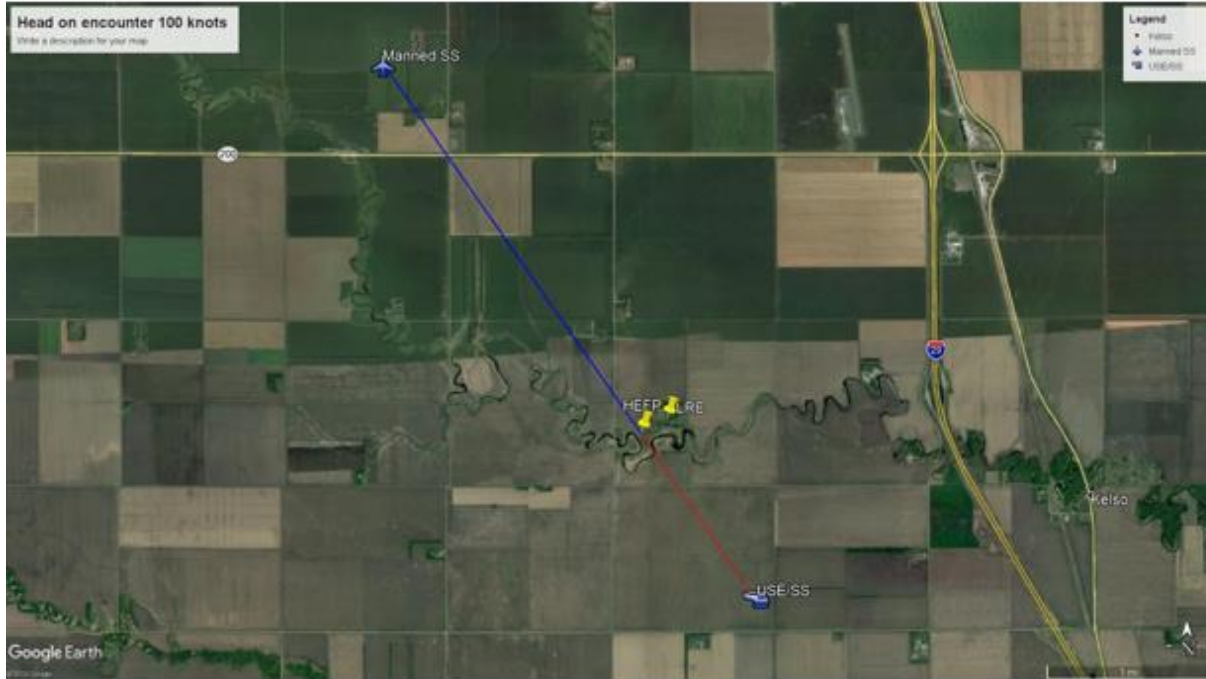
DAA System ID	L3Harris GBDAA	
DAA Sensors	Xtend ADS-B Receiver, C-Speed Radar, FAA NextGen (VAS)	
Supporting Technology	NPUASTS trailers, visualization systems, additional ADS-B receivers, video cameras, DCAPS data recording	
Intruder Pilot		
RPIC		
VOs		
MC		
FD		
COA/Waiver(s)		

Condition # (objective)				
✓	Action	Remarks	Call	Time
1a	UA maintains position at defined stand-off location ~6456 ft (~1.22 mi) from the Horizontal Encounter Focal Point (HEFP) as manned aircraft flies loop away from encounter location to set-up (S) for this encounter.	Point A 47.312755°, -97.072817°	RPIC calls "holding at point A"	
1b	Intruder executes turn at defined ground point ~14,346 ft (~2.71 mi) from HEFP during (S).	This is driven by the DAA technology, the warning/alert system, and UA speed. 47.359589°, -97.121141°	Intruder calls "Holding NW"	
1c	Intruder begins flying straight along its encounter path towards Scenario Start (SS).			
1d	UA exits (S) and proceeds towards SS once intruder exits its set-up turn.		Flight test director calls UA set up exit (USE).	

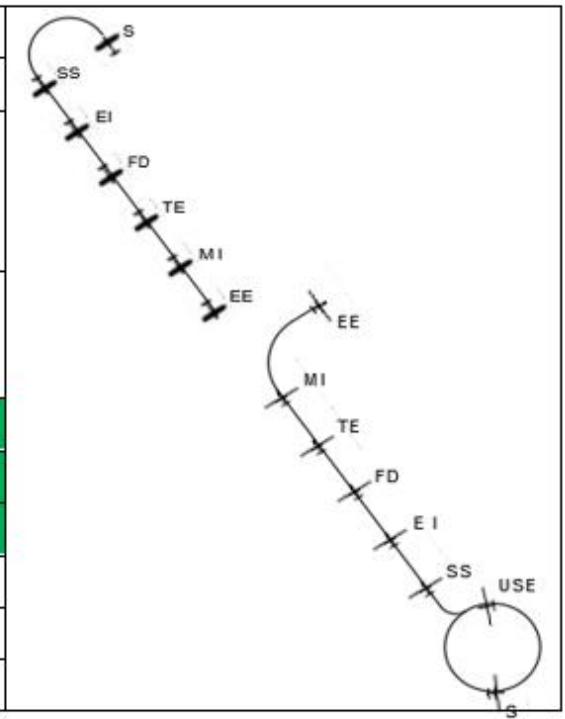


1e	Intruder varies speed to ensure arrival at HEFP within tolerance.			
1f	Altitudes are checked through radio calls.			
2	Arrival time at the HEFP is within tolerance—Scenario Start (SS) is declared.	Difference between arrival times at HEFP is ≤ 6.5 s.	Flight test director calls SS.	
3	Encounter Initiation (EI) is declared.	Occurs after SS and no later than approximate time of first alert or warning.	Flight test director calls EI.	
4a	Time of First Detection (FD) is recorded.	Data collector records the time of FD. If FD does not occur, this is noted.		
4b	Time of Track Establishment (TE) is recorded.	Data collector records the time of TE. If TE does not occur, this is noted.		
4c	Time of Maneuver Initiation (MI) is recorded.	Data collector records the time of MI. If MI does not occur, this is noted.	RPIC calls "maneuvering"	
4d	Approximate time of CPA is recorded.	If a maneuver occurs, data collector records approximate time of CPA. Exact time is determined with post-processing.		
4e	Well clear status recorded.	If known, data collector records status (maintained or not).		
4f	Regain well-clear time recorded	If well clear is not maintained, data collector records approximate time it is regained. Exact time is determined with post-processing..		
5	Encounter End (EE) is declared.	Data collector records the time of encounter end (same as scenario end).	Flight test director declares EE.	
6	Both aircraft proceed to set-up (S) for next encounter (if applicable).			

UAS Test Card



Flight Card #	A18-ND-UAS-HE-0-100
Date/Time	
Objective	Primary: Secondary:
Description	Manned aircraft and UAS encounters are conducted at the indicated cruise speeds. A vertical offset of 300' used to provide safety margin.
UAS Platform	FX 20
UAS Altitude	390 ft
UAS Speed	45 knots
Intruder	C150
Intruder Altitude	750 ft
Intruder Speed	100 knots





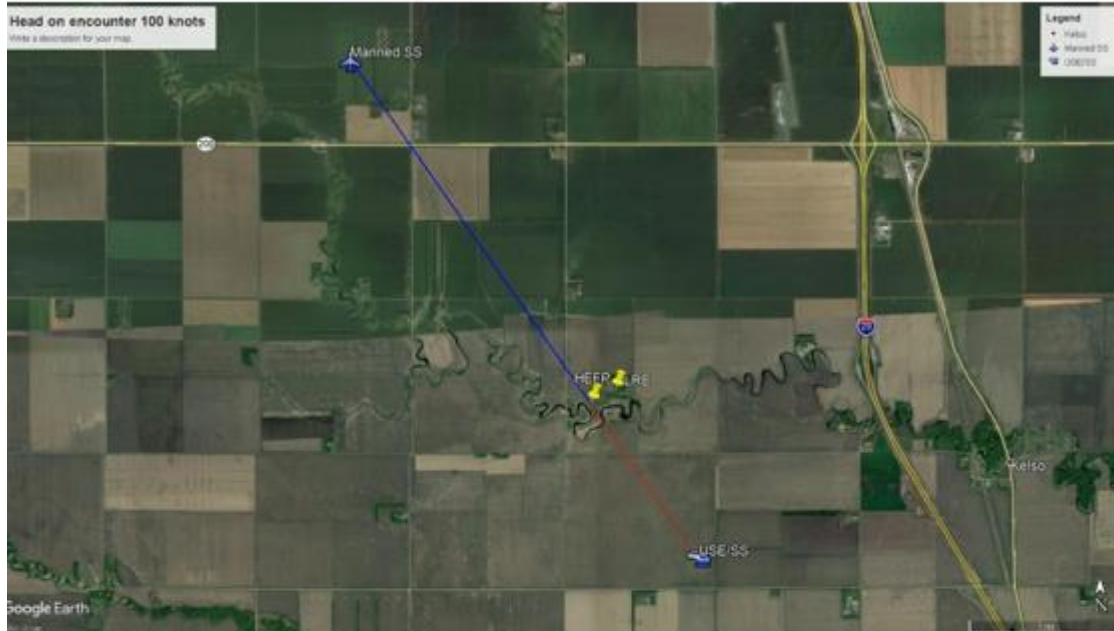
Location	47.328505, -97.087696. Lovas Farmstead.	
GCS	Mission Planner	
DAA System ID	L3Harris GBDAA	
DAA Sensors	Xtend ADS-B Receiver, C-Speed Radar, FAA NextGen	
Supporting Technology	NPUASTS trailers, visualization systems, additional ADS-B receivers, video cameras, DCAPS data recording	
Intruder Pilot		
RPIC		
VOs		
MC		
FD		
COA/Waiver(s)		

Condition # (objective)				
✓	Action	Remarks	Call	Time
1a	UA maintains position at defined stand-off location ~6456 ft (~1.22 mi) from the Horizontal Encounter Focal Point (HEFP) as manned aircraft flies loop away from encounter location to set-up (S) for this encounter.	Point A 47.312755°, -97.072817°	RPIC calls "holding at point A"	
1d	UA exits (S) and proceeds towards SS once intruder begins exits its set-up turn.		Flight test director calls UA set up exit (USE).	
1f	Altitudes are checked through radio calls.			
2	Arrival time at the HEFP is within tolerance—Scenario Start (SS) is declared.	Difference between arrival times at HEFP is ≤ 6.5 s.	Flight test director calls SS.	
3	Encounter Initiation (EI) is declared.	Occurs after SS and no later than approximate time of first alert or warning.	Flight test director calls EI.	
4c	Time of Maneuver Initiation (MI) is recorded.	Data collector records the time of MI. If MI does not occur, this is noted.	RPIC calls "maneuvering"	
5	Encounter End (EE) is declared.	Data collector records the time of encounter end (same as scenario end).	Flight test director declares EE.	



	6	Both aircraft proceed to set-up (S) for next encounter (if applicable).			

INTRUDER Test Card



Flight Card #	A18-ND-MAN-HE-0-100	
Date/Time		
Objective	Primary: Secondary:	
Description	Manned aircraft and UAS encounters are conducted at the indicated cruise speeds. A vertical offset of 300' used to provide safety margin.	
UAS Platform	FX 20	
UAS Altitude	390 ft	
UAS Speed	45 knots	
Intruder	C150	
Intruder Altitude	750 ft	
Intruder Speed	100 knots	



Location	47.328505, -97.087696. Lovas Farmstead.
GCS	Mission Planner
DAA System ID	L3Harris GBDAA
DAA Sensors	Xtend ADS-B Receiver, C-Speed Radar, FAA NextGen (VAS)
Supporting Technology	NPUASTS trailers, visualization systems, additional ADS-B receivers, video cameras, DCAPS data recording
Intruder Pilot	
RPIC	
VOs	
MC	
FD	
COA/Waiver(s)	

Condition # (objective)				
✓	Action	Remarks	Call	Time
	1b Intruder executes turn at defined ground point ~14,346 ft (~2.71 mi) from HEFP during (S).	This is driven by the DAA technology, the warning/alert system, and UA speed. 47.359589°, -97.121141°	Intruder calls "Holding NW"	
	1c Intruder begins flying straight along its encounter path towards Scenario Start (SS).			
	1e Intruder varies speed to ensure arrival at HEFP within tolerance.			
	1f Altitudes are checked through radio calls.			
	2 Arrival time at the HEFP is within tolerance—Scenario Start (SS) is declared.	Difference between arrival times at HEFP is ≤ 6.5 s.	Flight test director calls SS.	
	3 Encounter Initiation (EI) is declared.	Occurs after SS and no later than approximate time of first alert or warning.	Flight test director calls EI.	
	4c Time of Maneuver Initiation (MI) is recorded.	Data collector records the time of MI. If MI does not occur, this is noted.		
	5 Encounter End (EE) is declared.	Data collector records the time of encounter end (same as scenario end).	Flight test director declares EE.	



	6 Both aircraft proceed to set-up (\$) for next encounter (if applicable).			
--	--	--	--	--